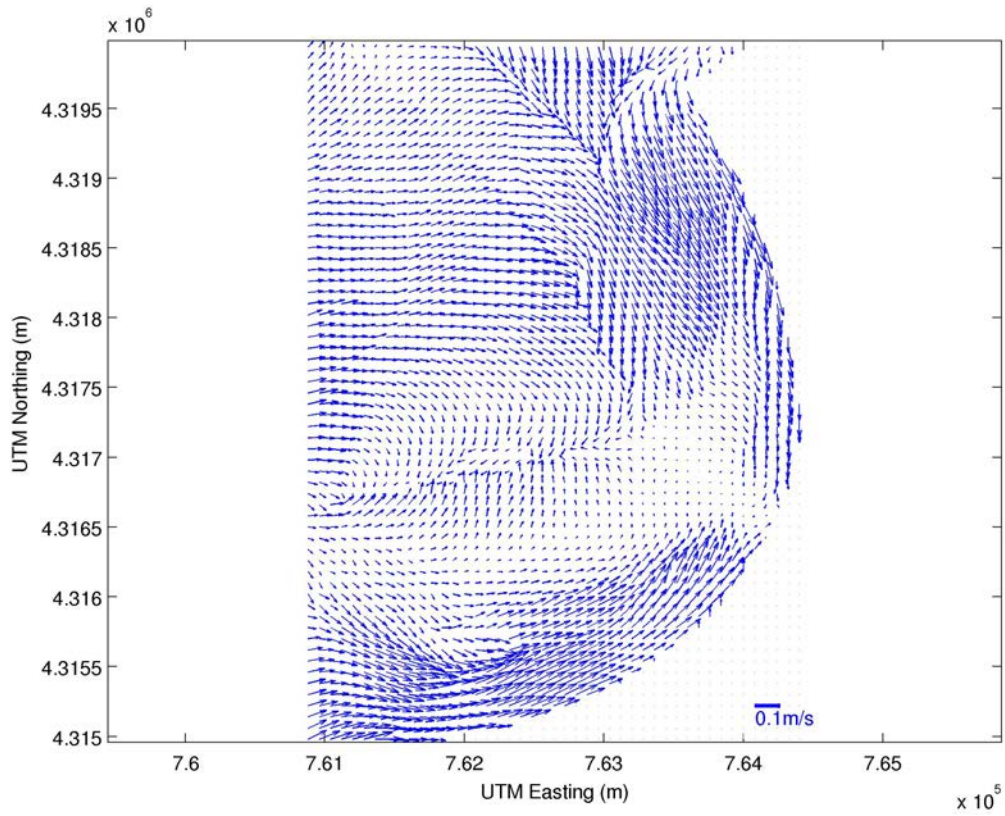# LAKE TAHOE FLOW MODELING, POTENTIAL PATHOGEN TRANSPORT AND RISK MODELING

S. Geoffrey Schladow, Andrea Hoyer, Francisco Rueda and Michael Anderson

June 2014

Cover Image - Surface current velocity shown at every 4th grid cell in the current model. The model grid cells are spaced every 20 m horizontally, so the velocity arrows shown are spaced every 80 m (260 ft.). The model result shown is for July 31, at 11 pm. Of particular note is the convergence of the currents, with a strong 0.1 m/s (1220 feet/hour) current down the east shore and a similar eastward current along the south shore.

Table of Contents

Executive Summary

Swimming and other body-contact recreational activities have been identified by the USEPA, the Nevada Division of Environmental Protection, the California Department of Health Services, and other public health professionals as a potential source of microbiological contamination of recreational waters. This study was undertaken to quantify the impacts of body-contact recreation on microbial water quality at the Kingsbury General Improvement District (KGID) and Edgewood Water Company intakes on Lake Tahoe. This study builds upon the risk assessment conducted previously (Black and Veatch, 2008), and specifically incorporates 5 new features: (i) findings of new 3-D hydrodynamic simulations for the nearshore southeastern portion of Lake Tahoe; (ii) development of a finer-scale 50 m x 50 m finite-segment pathogen fate-consumer risk model; (iii) additional recreational use associated with the proposed Beach Club and Edgewood Lodge/Resort developments; (iv) risk assessment for the Edgewood Water Company intake; and (v) treatment plant upgrades at KGID and Edgewood that include UV disinfection meeting the requirements of the Long Term 2 Enhanced Surface Water Treatment rule (LT2). As in the prior study, this risk assessment focused on Cryptosporidium because of its low infectious dose, environmental persistence and resistance to conventional disinfection. Mean annual Cryptosporidium concentrations were predicted using a Monte Carlo-based pathogen fate-consumer risk model. Dose-response calculations applied to predicted concentrations following treatment provided probabilistic estimates of health risks resulting from consumption of recreationally-impacted treated drinking water.

Model simulations demonstrate that the additional recreational use at Beach Club and Edgewood Lodge/Resort beaches, in conjunction with improved understanding of transport, results in increased potential for Cryptosporidium to reach the KGID and Edgewood intakes. For example, the median annual concentration at the KGID intake increased from 0.0018 oocysts/100 L (Black and Veach, 2008) to 0.0082 oocysts/100 L, although the additional 3-log removal achieved with UV disinfection following ozonation greatly lowered treated water concentrations and substantially lowered risk of infection. The predicted median annual risk of infection was lowered from 0.23 (Black and Veatch, 2008) to 0.0011 infections/10,000/yr (this study) for KGID, while the probability of exceeding the USEPA target of 1 infection/10,000/yr was reduced from 4.9% (Black and Veatch, 2008) to <0.02 infections/10,000/yr (the lowest probability limit based upon the number of simulations). The median predicted annual risk level for the upgraded ozone+UV Edgewood plant was 0.0007 infections/10,000/ yr, with <0.02% probability of exceeding the USEPA target (lowest probability limit).

The modeling results that underpinned these conclusions provide a number of additional insights to minimizing pathogen entrainment into drinking water intakes. Primarily, by using a technique developed under this project, it is now possible to determine the source area of pathogens (or any other contaminant) that arrive at a water intake. The results also provide insight into the complex interplay between the windfield, the strength of the lake's thermal stratification and the transport patterns of pathogens. Most notably, having an intake located below the maximum depth of the thermocline greatly reduces the frequency of pathogen arrival at the intake. This has other implications with respect to lake level and drought conditions. With prolonged drought episodes (predicted to be more frequent under future climatic conditions), lake level will be lower and thereby reduce the depth of the water intakes. Under those conditions the period of time favorable for pathogen transport to the intakes is likely to increase

significantly. Similarly, the time of water withdrawal can be used to minimize risk. Night time and early morning withdrawals seem to pose the greatest risk, as pathogens released the previous day have had little opportunity to be de-activated by solar radiation. This highlights the linkage between drinking water quality and maintenance of high water clarity, particularly in the nearshore region. Maximizing the penetration of UV radiation from solar radiation into the water column provides "free" water treatment.

The release of a surrogate for herbicide transport from the vicinity of Tahoe Keys was simulated, and showed that herbicide could be transported to the vicinity of the nearshore regions of south-east Lake Tahoe within a 24 hour period. Within that period, material did not actually arrive at any of the water intakes, but based on other results in this report, that would occur within less than 48 hours. It must be borne in mind that these results are a first estimate of the fate of herbicides. No account has been taken of the dilution that a real plume of herbicide would be subject to, and the possible breakdown into other chemicals. Likewise the toxicity (if any) of the herbicide for the case of consumption or body contact recreation has not been considered as it was beyond the scope of the study. However, should the use of herbicides be permitted at Lake Tahoe, there is a strong case that a more complete study of the fate of these products on public health should be undertaken.

1. Introduction

The Long-Term 2 Enhanced Surface Water Treatment Rule (LT2 rule) was specifically developed by the USEPA to provide additional consumer protection against Cryptosporidium and other disease causing microorganisms in drinking water drawn from surface water or ground water under the direct influence of surface water, especially unfiltered systems and filtered systems with high levels of Cryptosporidium in their source waters. The LT2 rule requires unfiltered systems to meet treatment technique requirements for Cryptosporidium no later than October 1, 2014. Incline Village General Improvement District has upgraded the Burnt Cedar water treatment plant to include UV treatment, while KGID, Edgewood, Glenbrook and Zephyr Water Utility District are completing construction of new ozone/UV water treatment plants. These improvements are thus expected to markedly improve the quality, safety and reliability of drinking water for their customers.

At the same time, however, two significant development projects are planned near/within the shorezone adjacent to the KGID and Edgewood Water Company's intakes: the Edgewood Lodge and Golf Course Improvement Project with new public beach and relocated-expanded pier, and the Beach Club and associated beach on Lake Tahoe. This study was undertaken to assess the cumulative impacts on finished drinking water quality and consumer public health due to increased recreational use near the KGID and Edgewood intakes and treatment plant upgrades required by LT2.

The present study represents a considerable advance in the ability to assess health risks associated with pathogen release in drinking water sources since a previous study at Lake Tahoe (Black & Veatch, 2008). The advances primarily relate to improvements in the spatial resolution of the numerical models that are the basis of such assessments. At the time of the previous study, the three-dimensional flow fields that were required to provide necessary water velocity estimates had a spatial resolution of 500m. The present version of the model has reduced this spatial resolution to 20 m. The pathogen fate-consumer risk model also had a correspondingly finer scale of 50 m. This is particularly important in the shallow, nearshore regions where body contact recreational activities and drinking water intakes are located.

The report has been organized to correspond to the three specific tasks that needed to be addressed. The tasks were as follows:

Task I: Lake Tahoe Flow and Particle Modeling
Produce a refined three-dimensional hydrodynamic flow model for Lake Tahoe. The "coarse grid" model will have a horizontal grid size of 100 m. Within this "coarse grid" model a nearshore "fine grid" sub-models will be implemented in all areas relevant to the goals of this study, including the full spatial extent of water intake structures. The horizontal grid size of the "fine grid" will be 20 m. The time-varying current field within each cell of the "fine grid" model for a representative summer period will be utilized as input to Task II. Maps showing current patterns within the nearshore region adjacent to the project area will also be produced.

Task II: Intake-Specific Flow and Risk Modeling

Update the risk model for the Probability of Infection, focusing on Cryptosporidium, using the more refined localized 20 meter grid system developed under Task I. The model will be applied for the KGID intake and the Edgewood intake by including, at minimum, the new potential contaminating activities associated with approved public beach areas at Edgewood Golf Course, located adjacent to the Edgewood intake, and at the Beach Club, located adjacent to the KGID intake.

Task III: Potential Threat from Herbicide/Pesticide Use
Utilizing the updated hydrodynamic model, run several scenarios of the release of herbicide/pesticide from any point in the lake and to analyse the results.

Each Task has been written up as a largely standalone report. However, the results are connected, in that results presented under Tasks II and III are dependent on the results achieved in Task I. Hoyer, Schladow and Rueda were primarily responsible for Tasks I and III. Anderson was primarily responsible for Task II. For Task I, in addition to producing the water current magnitudes required to conduct Task II, a new approach to assessing pathogen risk has been developed, through which the source area from which pathogens originated can be determined for any specific water inlet. The approach was demonstrated using a hypothetical water intake but for pathogen loads consistent with the recreational areas of the southeast corner of Lake Tahoe.

2. Lake Tahoe Flow and Particle Modeling

2.1 Methods

2.1.1 Approach

A 3D Lagrangian, individual-based particle model developed by Hoyer et al. (2014a) was modified to develop a novel method to assess the risk of pathogens entering the drinking water supply from intakes in a lake, hereafter referred to as the pathogen model. Unlike the conventional approach where pathogens are tracked from a point of origin, the velocity fields are inverted and the points of origin of individual pathogens are calculated by back-tracking their individual trajectories from the area of withdrawal.

These simulations are driven by lake current and turbulence simulations conducted with a 3D hydrodynamic model. The lake currents and diffusivities were computed using a parallel version (Acosta et al. under review) of the 3D Cartesian hydrodynamic model of Smith (2006). The model solves the 3D form of the shallow water-wave equation, and has been extensively validated both against analytical solutions (Rueda and Schladow 2002; Rueda et al. 2003) and field data sets (Rueda and Schladow 2003; Rueda and Cowen 2005; Rueda et al. 2008). The transport and mixing model is a truly dynamic model that predicts the changes in the hydrodynamic conditions of the lake every 50 seconds (hydrodynamic time step).

The model was forced using sequences of spatially variable wind fields, constructed through spatial interpolation of 10-minute wind records collected at 10 stations around the lake (Barnes 1964). The model's horizontal grid was 100 m x 100 m in coarse mode, with embedded 20m x 20 m fine grids. This grid resolution was a compromise between the need to adequately resolve motions within small embayments and the computational cost. The bathymetry was a modified form of Gardner et al. (1998). The vertical resolution in the hydrodynamic model was variable, ranging from $\Delta z = 0.5$ m at the surface to $\Delta z = 10$ m near the bottom (at a depth of 500 m). The initial temperature profile was obtained from thermistor-chain records (thermistors located at 5, 10, 15, 20, 25, 30, 40, 60, 80, 100, 120, 140, 180, 200, 240, 280, 320, 360, 400 and 440 m depth) interpolated to the vertical grid spacing. The 3D hydrodynamic model was used to produce velocity fields, examples of which are included in this chapter. Velocity records produced by the model were also used as the basis of the formal risk assessment in Chapter 3.

This technique is computationally efficient. The non-point source nature of pathogens released by body-contact recreation would require a large number of simulations from different beach areas, containing many potential points of origin. In contrast, the knowledge of the point of concern (the water intake) makes it possible to consider only those (simulated) pathogens originating from source areas (recreational beaches) that reach the water intake. In the following, the term 'particles' refers to all individual particles simulated by the model, while 'pathogens' are those particles that were predicted to originate from recreational beaches. The validation of the hydrodynamic model has been previously described (Hoyer et al. 2014b). The simulation results permitted the establishment of the risk patterns, their temporal variations and the link existing between risk and local lake circulation and stratification dynamics. Although this study focuses on *Cryptosporidium*, the generic pathogen dispersion model may be applied to any other pathogen, such as for example *Giardia* spp., as well as bacteria and viruses.

2.1.2 Pathogen model

The pathogen model consists of a Release-module, a Transport-module and a Survival-module. The modules run sequentially and independently of each other. The model is driven by external computations that simulate hydrodynamic conditions prevailing in the lake. A Cartesian grid formed the domain for all simulations. A detailed description of the pathogen model and the links between the different modules and external computations can be found in Hoyer et al. (2014a).

The **R**elease–module (or R-module) simulates the process of pathogen release into the water column by body contact recreation. Pathogens may be released from skin surface during contact with water (shedding) and through accidental fecal release (AFR). The number of oocysts released by recreators at an instant of time t, $N(t)$, is given by (Anderson et al. 1998)

$$N(t) = R(t) \cdot \left(IM_S C_P + IFM_A C_P \right)$$

Here I is the average infection rate (%) and M_S represents the mass of fecal material shed by a recreator (g recreator^{-1}). C_P is the pathogen content of the fecal material (number of pathogens g^{-1}), F is the rate of AFR, and M_A is the mass of AFR (g recreator^{-1}). These parameters are taken to be constant over time. The mean recreators density, $R(t)$ (recreator m^{-2} d^{-1}), is variable in time, indicated by index t, being typically higher at weekends than at week days.

Beach areas may be defined by substrate (sand) and a critical water column depth H_{cr}. Only those grid cells that are equal or lower then H_{cr} ($H \leq H_{cr}$, where H=water column depth at cell(i,j) and $H_{cr}=2m$) are considered to be contributing pathogens released by recreators into the water column. Pathogen release was assumed to occur during the day by recreators and during night time from the sediments through resuspension (Wu et al. 2009, Abdelzaher et al. 2010). The solution of the module consists of a time series of number of pathogens released into the pelagic over a given time period tl.

The **T**ransport-module (or T-module), simulates the pathways of released pathogens between beach areas and water intakes. Time varying 3D velocity fields and vertical diffusivity profiles from the external hydrodynamic computations are the drivers of these simulations. The simulations of the T-module are carried out using a Lagrangian model. In this model, particles are free to move independently of the model grid. However, the underlying hydrodynamic information (i.e. 3D velocity field, vertical eddy diffusivity, and temperature) is provided as input to the model based on the Cartesian grid and then interpolated to the particle position. For a detailed description of the 3D time-varying particle tracking model see Rueda et al. (2008). Pathogens are treated as free particles in accordance with their strongly negative surface charge (at neutral pH) and their resistance to form aggregates with natural soil particles (Ongerth and Pecoraro 1996, Dai and Boll 2003, Dai et al. 2004) or organic particles (Brookes et al. 2004b). Particles are back-tracked from the intake to their points of origin. This back-dispersion method comprises calculating the particle displacement at each time step from (a) the inverted 3D velocity field and (b) a random component representing the effect of horizontal and vertical diffusion (Han et al. 2005). Transport simulations start every Δt_0 with the release of N_0 particles from the source cell (i_0, j_0) at time t_0 that are tracked during a period of ΔT. Pathogens infectivity is known to be sensitive to solar radiation in the ultraviolet (UV) wavelengths (Häder 2003,

Betancourt and Rose 2004, and references therein). The most energetic and damaging part of the UV spectrum, UV-B radiation (290-315nm), is approximately 1% of the global radiation (Grant et al. 1997). The UV-B radiation reaching a given individual l at time t is calculated from its vertical position z (l, t), below the surface, and from the incident short wave radiation reaching the free surface $I_0(t)$ (Wm^{-2}), as follows,

$$I(l,t) = 0.01 \cdot I_0(t) \cdot \exp\left[-k_{UV}(t) \cdot z(l,t)\right]$$

Here $k_{UV}(t)$ is the constant (in time and space) light attenuation coefficient set to 0.15 m^{-1} (Rose et al. 2009). The time-dependent light intensity reaching a given particle is then used to calculate the light dose over a given time period. The light dose experienced by the individual l, as it travels, $ID(l, t)$ (Jm^{-2}), is calculated as the amount of energy received, as follows

$$ID(l,t) = \sum_{t_0}^{t} I(l,t) \cdot \varDelta t_T$$

Here Δt_T is the time step of the transport module. Note that the dose is a cumulative variable, and provides a measure of the energy that a given individual may have received, from time t_0 when it was at the intake to the time t it reaches a source beach site (i,j), t_s ($t=t_s$). The solution of each of these model runs consists of the temporally varying position of the N_0 particles during time interval ΔT and the history of environmental conditions (temperature and solar radiation) that acted on each individual during its journey.

The **S**urvival-module (or S-module) accounts for the survival/inactivation of pathogens during their transport subject to the environmental conditions recorded in the **T**-module. Particles withdrawn at the intake are considered to be pathogens released by recreators if (a) they originate from a swimming beach and (b) if the environmental conditions endured during their journey do not affect their survival (infectivity). Therefore, the probability P_V of a given intake to be contaminated by pathogens released at any beach source B at an instant of time t is expressed as the product of the probability of beach origin P_B and the probability of survival P_S

$$P_V = P_B \times P_S \tag{4}$$

The probability of beach origin P_B is the fraction of withdrawn particles that originate from beach source areas identified by substrate type (sand) and water column depth H. Here H must be lower than or equal to a critical depth H_{cr} ($H \leq H_{cr}$). The probability that a pathogen remains viable or infectious, P_S, in the presence of the water temperatures and solar radiation endured is expressed as

$$P_S = P_T \times P_I \tag{5}$$

The probabilities P_T and P_I correspond to temperature and light, respectively. The probability of survival due to water temperature, P_T, is calculated from the temperature inactivation rate proposed by Walker and Stedinger (1999)

$$P_T = 1 - (10^{-2.68} \cdot 10^{0.058\theta})$$

The probability P_T is evaluated for the mean temperature θ over the time it takes for a given particle to travel from the beach area to the intake. Pathogen inactivation due to solar radiation is defined in terms of infectivity. A given pathogen is considered inactivated when it receives a light dose sufficiently high to inhibit cell division and, hence, infectivity – though it may still be viable (Monis et al. 2014). For simplicity, the light dose necessary to reduce pathogen infectivity to 0.01% (4-log inactivation), ID_{99}, is taken as a critical value and all particles that receive this dose are deemed to be inactivated. This approach may overestimate the number of infectious pathogens, compared to a probability density function, and may be considered to represent the worst-case scenario. The solution of the S-module is a time series of the probability of pathogens to be withdrawn at the intake, calculated every Δt_0 seconds. Here, the pulses of withdrawn pathogens at time t represent the fraction of infectious pathogens originating from recreational beaches.

2.1.3 Application to Lake Tahoe

The pathogen dispersion model was applied to *Cryptosporidium* in Lake Tahoe during a 2 month summer period, from July 1 (Day 183) to August 27 (Day 240), 2008 (the study period). The location of the drinking water intake and known beach areas that may be potential sources of pathogens to the intake are indicated in Fig.1b. The recreator density was assumed to be 0.01 ind.m^{-2}d^{-1} during weekends, and 60% of that value on week days. In spite of reports on different infection rates between children and adults (see Gerba 2000 and references therein), daily age-structured observations of bathers are difficult to obtain and an average value was utilized. The infection rate I was assumed to be 3% (Anderson et al. 1998, Gerba 2002) with a mass of fecal material shed M_S of 0.1 g/recreator (Gerba 2000). *Cryptosporidium* mean contents of feces were set at 10^6 oocysts g^{-1} feces (Jakubowski 1984, Robertson et al. 1995). Accidental fecal releases were assumed to occur for 1 in 1000 bathers, $F=10^{-3}$ (Anderson et al. 1998) and a mass M_A of 125g/AFR (Feachem et al. 1983, Bitton 1994).

The intake was assumed to be at a water depth of 15.85 m (52 ft) and 1.8 m (6 ft) above the lake bed. The intake pumping rate was considered continuous at a value of 18 Ls^{-1} (4.76 gal. s^{-1}). Particle releases commenced five days after the beginning of the hydrodynamic simulations, at day 188, to allow the hydrodynamic information to depart from the initial conditions (model spin up). In the T-module, a normal-distributed particle cloud was initialized at the intake on an hourly basis (Δt_0 =1h), centered at the intake with a standard deviation of σ_{xy}=40 m (two horizontal grid cells) and σ_z=0.2m in the horizontal and vertical, respectively. The module was then run backward in time with a time step Δt_T =10s, to satisfy the convergence criterion for particle tracking simulations (Ross and Sharples 2004). The transport simulations were driven using velocity and diffusivity fields from the hydrodynamic model. The hydrodynamic information and simulated temperature was given to the T-module every 3600s ($\Delta t_{h\text{-}output}$ = 1h) and interpolated to Δt_T. Solar radiation data at 10 minute intervals was also passed to the T-module backward in time to estimate UV exposure. The number N_0 of particles released in each T-simulation was set to 10^3, to guarantee feasible computational costs. A single settling velocity w_s= 10^{-7} ms^{-1} was defined based on the value for *Cryptosporidium* predicted by Stokes' law (Yates et al. 1997) and supported by empirical estimates (Medema et al. 1998, Dai and Boll 2006). For the back-dispersion simulations, the settling velocity was inverted to become a buoyancy velocity. The simulations ended when at least 99% of the particles reached a light dose three-fold the critical value for 99.99% inactivation, ID_{99} (in terms of infectivity), i.e. 3xID_{99}..

Generally, this criterion was met within a time period $T \leq 1$d. The inactivation dose ID_{99} was defined based on empirical values found in the literature (Rochelle et al. 2005, Connelly et al. 2007, King et al. 2008). Most studies on *Cryptosporidium* inactivation have focused on the UV-C radiation of 254nm (e.g. Craik et al. 2001, Morita et al. 2002, Hijnen et al. 2006) and found ID_{99} of $O(10)$-$O(10^2)$ Jm^{-2}. Given that UV-C radiation is attenuated in the atmosphere before reaching the earth surface and that UV-B radiation is of larger and less energetic wavelength, the critical light dose ID_{99} was conservatively taken to be one order of magnitude higher, $ID_{99} = 10^3$ Jm^{-2}.

2.2 Hydrodynamic simulations

The hydrodynamic simulations of lake currents and mixing variables were carried out using a parallel version of the semi-implicit 3D hydrodynamic model of Smith (2006) (Acosta et al. 2010), and based on the numerical solution of the 3D form of the shallow water equation. The high-resolution hydrodynamic simulations were carried out in a two step nested procedure: In the first step, the whole lake domain was run with low spatial resolution, on a 100m grid in both the EW and NS directions. This model run produced the boundary conditions for the high resolution simulation. In the second step, these boundary conditions were used to run a reduced domain of the lake (Fig.1b) on a 20m horizontal grid. The vertical resolution was variable, ranging from $\Delta z = 0.5$ m at the surface to $\Delta z = 10$ m near the bottom (i.e. at a depth of 500 m) and equal for both horizontal resolutions. The model was forced using surface heat and momentum fluxes derived from local atmospheric variables (short and long wave radiation, air temperature, relative humidity, and wind speed and direction) observed at 10 locations around the lake (Fig.1a). The interpolation method proposed by Barnes (1964) was applied to construct the spatially variable wind fields used to force the model. The bathymetry was based on Gardner et al. (1998). The time step of the hydrodynamic model was 50s and 10s for the 100m and 20m simulations, respectively. The horizontal eddy diffusivity K_h was set to 1 m²s^{-1} (100m grid) and 0.01 m²s^{-1} (20m grid). The initial temperature profile setup a stable stratification with a maximum of 19.75°C (surface) and a minimum of 5.12°C (hypolimnion) obtained from thermistor chain records (moored at T1, Fig.1a) at day 188 at 0000 hrs.

Current fields can be produced for any time and at any depth (or cross-section) desired. For illustration purposes, to show the extreme variability that characterizes the nearshore currents fields at Lake Tahoe, Fig. 2 shows the surface currents at 6 points in time.

2.3 New Risk Assessment Methodology Results
2.3.1 Pathogen sources

A very small percentage (0.02 %) of the water withdrawn during the study period was shown to originate from the shallow near-shore beach areas. Withdrawn water originated mainly (99.98%) from a depth below that associated with the shallow beach areas. There were days when 100% of the withdrawal originated from deeper waters, thus, assumed to be free from pathogens. In contrast, in extreme cases, up to 11% of the daily water volume was predicted to come from recreational beaches. Of the pathogens that reached the intake 81% originated from the beaches south of the intake and 19% from beaches north of the intake (Fig.3). These pathogens were transported by the currents in the coastal boundary layer that is part of a large scale cyclonic (counter-clockwise) gyre at the southern end of the lake (Hoyer et al. 2014b).
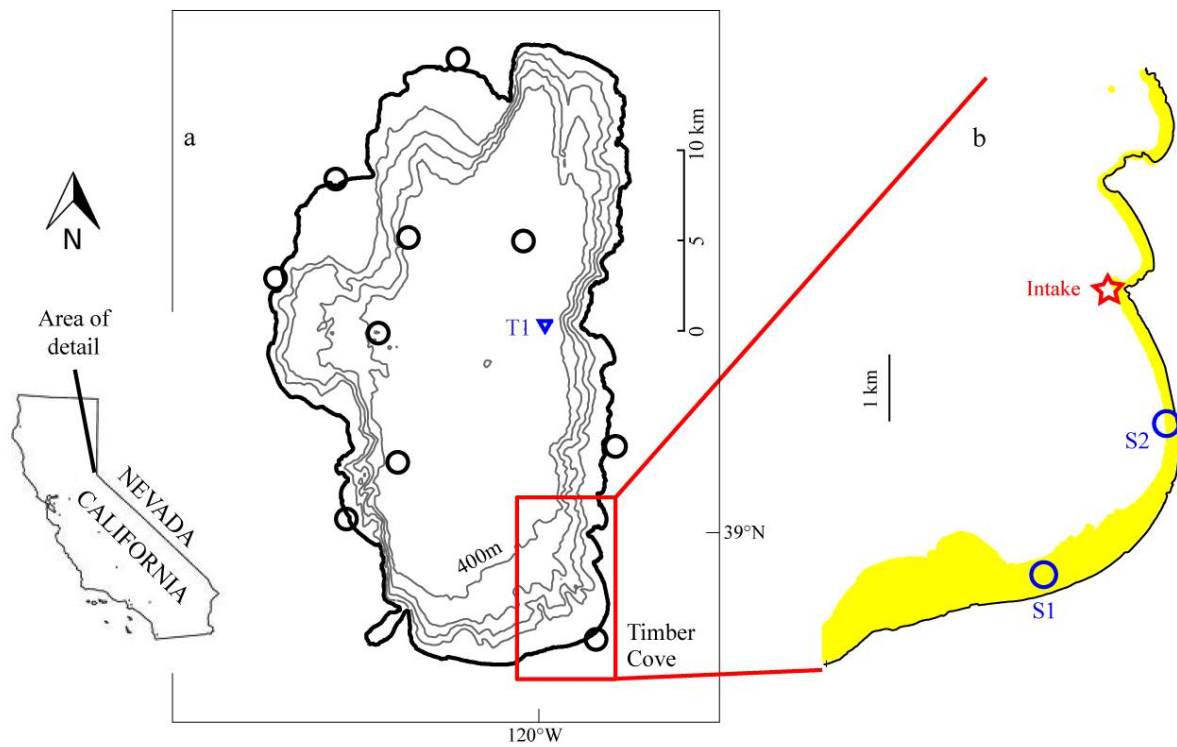
Flow Modeling and Pathogens
PO # S004422

Figure 1. Lake Tahoe: (a) location, bathymetry (at 100 m contour intervals) and location of meteorological stations (circles), initial temperature profile (triangle), and (b) area of interest: location of water intake (star), beach areas (yellow) and locations of simulated velocity output (circles).

(a)

Flow Modeling and Pathogens
PO # S004422

Flow Modeling and Pathogens
PO # S004422
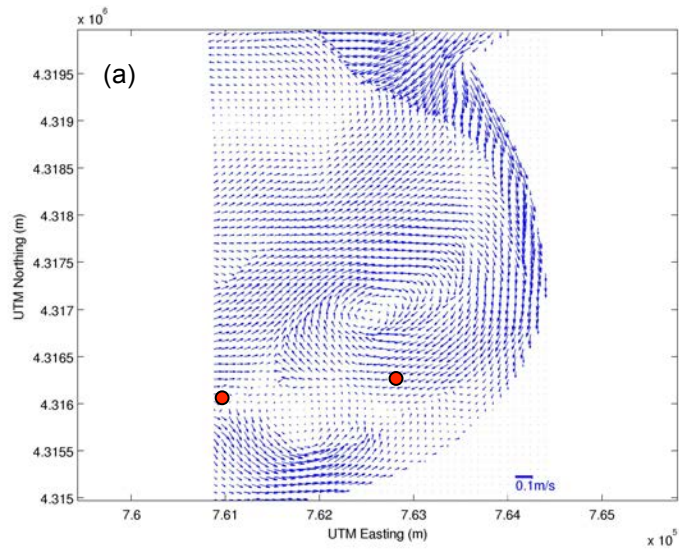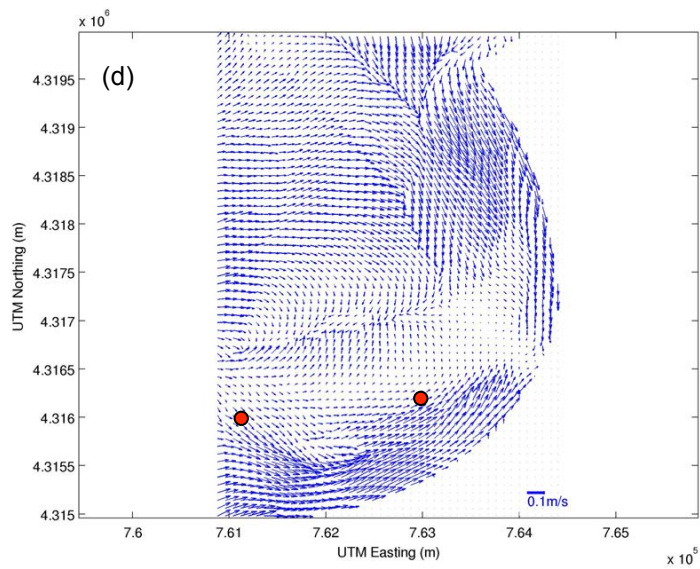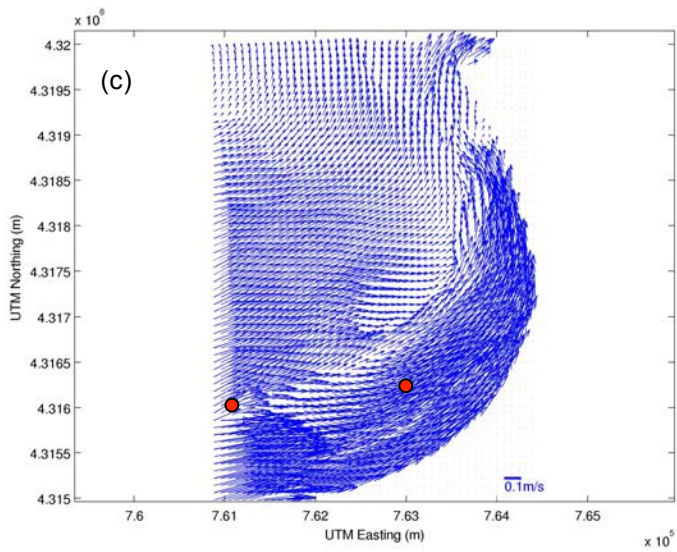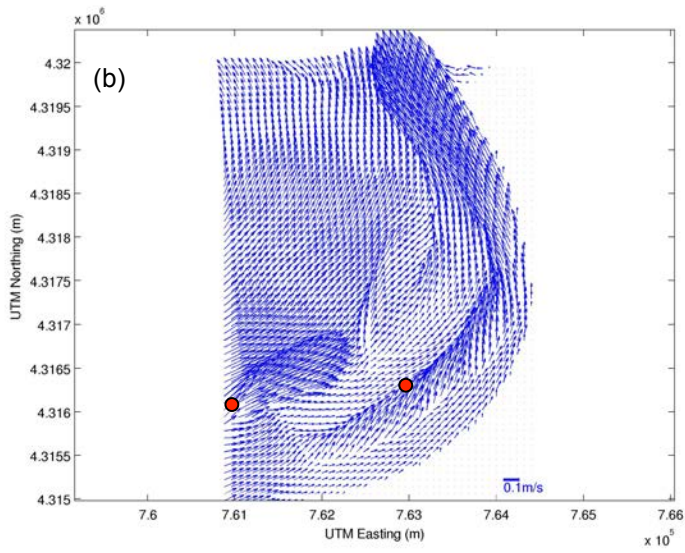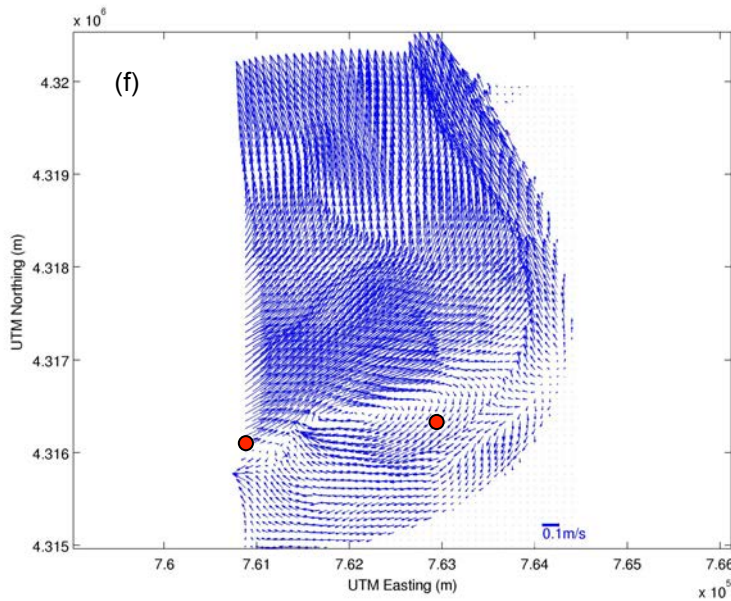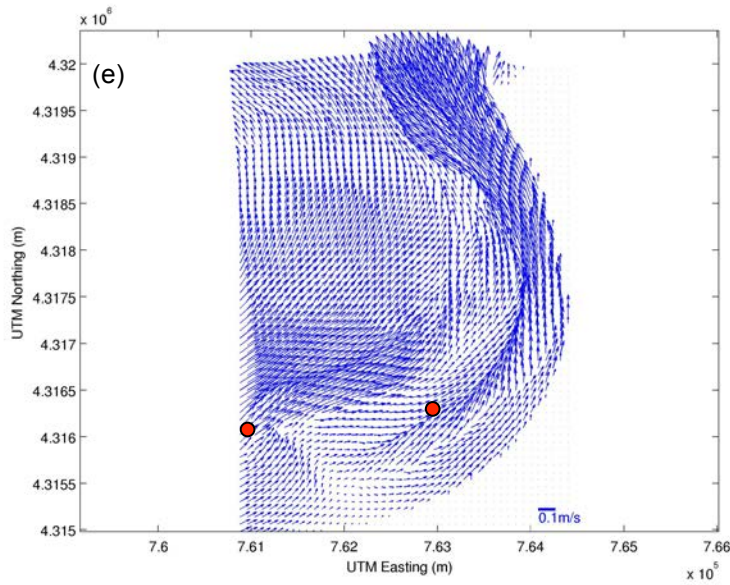
Figure 2. Surface currents vectors at every 4ᵗʰ gridpoint in the 20 m fine mesh at (a) July 28, Day 210, 1600h; (b) July 28, Day 210, 2300h; (c) July 29, Day 211, 1900h; (d) July 31, Day 213, 2100h; (e) Aug. 2, Day 215, 2300h; and (f) Aug. 4, Day 217, 0100h. The red dots indicate the locations of the Kingswood Grade General Improvement District's and Edgewood Water Company's water intakes.
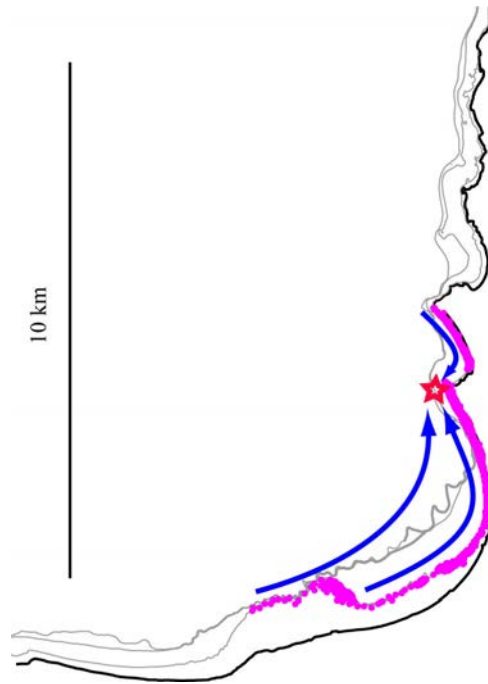
Figure 3. Distribution of pathogen sources over the study period (magenta). The magenta points correspond to all locations where the back-tracked particles first encounter a water depth of 2 m at a beach area over the entire simulation period. Star marks intake location of the Round Hill General Improvement District. Blue arrow mark pathways of dispersion. Depth contours (gray) show 2, 9, and 16m isobaths for orientation.

Overall, the near-shore circulation is driven mainly by the local winds acting on the lake surface. Moderate SE and strong SW winds at Timber Cove (Fig.4) induce persistent and strong northward currents along the southeastern shore that transport pathogens in the coastal boundary layer from the beach areas towards the intake (Fig.5a, b and c). High surface currents ($>0.1ms^{-1}$) are seen to occur nearly on a daily basis. Cross-shore currents at the intake were weaker than the alongshore currents, typical for flow in coastal boundary layers (Largier 2003, Rao and Schwab 2007, Nickols et al. 2012). The contrast between along-shore and cross-shore currents intensity was also seen at S2 (Fig.5b) and at S1 (Fig.5c). Daily alongshore currents exceeded 0.2 ms^{-1}, while across-shore currents where generally less than 0.05 ms^{-1}. Pathogens originating north of the intake were most likely to be transported to the south during the morning, when winds came from the NW (onshore winds due to land warming). These winds induced weak to moderate along-shore currents towards the intake (Fig.5a).

There were three main transportation pathways from the source areas to the intake (Fig.3): (i) southward along the shoreline of the bay north of the intake, (ii) northward along the south-eastern shore following the 2m contour, and (iii) northward, from the southern shore across the open water. Transport time from a beach to the intake varied from 1.7-24h depending on the point of origin and the local current velocities. The shortest transport times were observed

for pathogens released at the south-eastern beach area (1.7-22.8h) given its proximity to the intake and the elevated currents generated in the late evening (Fig.5b). Intermediate transport times were also observed for pathogens originating from beaches north of the intake (6.4-16.9h),
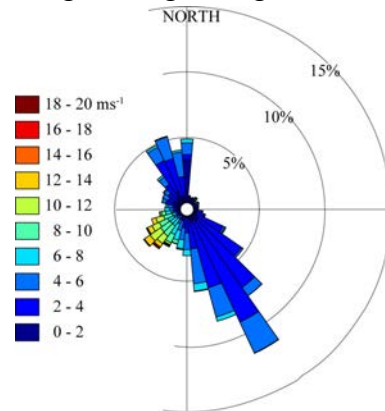
Figure 4. Wind speed and direction at Timber Cove (see Fig.1).
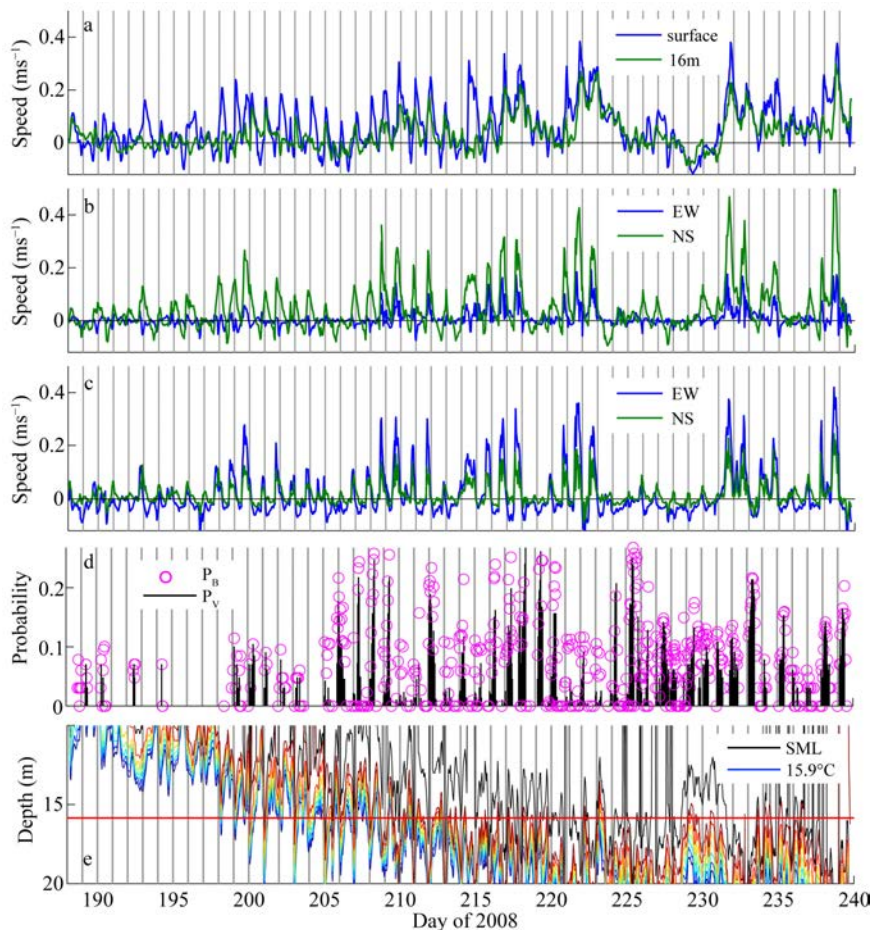
Figure 5. Simulated velocity currents at the intake (a) in the NS direction at the surface (blue) and 16m (green) depth, S2 (b) and S1 (c) in the EW (blue) and NS (green) direction at the surface. North and East are shown as positive. Probability of pathogens reaching the water intake PB (all pathogens) and PV (viable pathogens) (d). Depth of diurnal surface mixed layer (black line) calculated from simulated temperature and isotherms (colored lines) at the

mainly due to its proximity as southward currents were weak (<0.05ms^{-1}, Fig.5a). Pathogens released at the southern beach area had the highest range of transport times (2.2-24h).

2.3.2 Pathogen withdrawal

The probability, P_V, of withdrawal of pathogens at a given intake (the product of the probability of beach origin P_B and the probability of survival P_S) increased overall during the study period and varied on a daily basis, being highest at night and in the morning (0300-1200). Pulses of pathogens were predicted to enter the intake on a regular basis. During the study period, we discerned three phases in the amount and frequency of pathogens arriving at the intake. During phase 1, from day 188 to day 198, viable pathogens reached the intake episodically with a probability that viable pathogens will be withdrawn of $P_V<0.1$ during these episodes (Fig.5d). From day 199 to day 205 (phase 2), withdrawal of pathogens occurred almost on a daily basis with a probability P_V of up to 0.1 during episodes. After day 205 until day 240, (phase 3) pathogens were withdrawn regularly and at significantly higher amounts compared to phases 1 and 2. P_V reached daily maxima of 0.3 during this phase. Occurrence of pathogens occurred mainly between 0300 and 1200, with highest values at 1000. Between 0100 and 1000, almost all pathogens that reached the intake were active (or infectious). The highest numbers of inactivated pathogens were withdrawn between 1200 and 1400. The temporal variability of withdrawn pathogens during the day suggests that the pattern of pathogen withdrawal is controlled by the temporal dynamics of vertical dispersion associated with lake motions. The differences between active and inactivated pathogens that reach the intake indicates that these pathogens are highly sensitive to environmental conditions (temperature or light) endured during their journey toward the intake.

2.3.3 Pathogen vertical dispersion

The vertical dispersion of pathogens was tightly linked to the temporal dynamics of the depth of the surface mixed layer (SML), over which they are dispersed constantly and uniformly. The thermocline depth of Lake Tahoe ranged from 10-20 m during the study period (Fig.5e) and the stability of the water column was high. The Wedderburn number, W, and the Lake number, L_N, (Stevens and Imberger 1996), used to parameterize the balance between stabilizing thermal stability and destabilizing wind forcing, were both well above unity at all times. Assuming a two-layer stratification with an upper mixed layer of thickness H, the displacement of the interface, Δh, driven by wind forcing can be estimated as $\Delta h = 0.5H/W$ (Shintani et al. 2010). Interface displacement was of order 8m, suggesting that the intake at the 16m isobaths was at times within the SML.

The depth of the diurnal SML ranged between the near surface and the top of the metalimnion due to diurnal temperature variations (Fig.5e). The SML depth was calculated based on density differences, derived from the simulated temperatures time series at the location of the intake. A threshold value for the base of the SML was assumed to be a density gradient of 0.02 kg m^{-4} (Reynolds 1984). The depth, at which the density difference $d\sigma$ between the density σ_z and the surface density σ_0 yielded a linear gradient equal to 0.02 kgm[-4], was taken to be the depth of the SML. The three phases identified earlier can be related to the maximal depth of the diurnal

SML during night time cooling: (i) At the beginning of the study period, from day 188 to day 198 (phase 1), the SML was relatively shallow and deepened to a maximal depth of 10m (Fig.5e). During phase 2, the maximal depth of the SML during the night increased progressively from 10m to ~16m from day 199 to day 205, respectively. After day 205 until day 240 (phase 3), the depth of the SML exceeded 16m on a daily basis. Consequently, the intake (z = 15.85m) was located at or below the depth of the SML during 80% of the time during this phase. The deepening of the SML below the depth of the intake exposes the intake to surface (epilimnetic) waters, which are typically of lower water quality and may carry potential contaminants, such as human waterborne pathogens.

The vertical excursions of pathogens from the shallow beach areas to the intake depend on the vertical mixing intensities. *Cryptosporidium* oocysts with a settling velocity $w_s=10^{-7}$ ms^{-1}, typical from *Crytosporidium* (Dai and Boll 2006), are practically neutrally buoyant in turbulent environments. With a diurnal SML depth H of O(10)m, as predicted for Lake Tahoe, the vertical eddy velocity v_z ($=K_z/H$) is 10^{-7}ms^{-1} and of the same order of magnitude as the settling velocity of *Cryptosporidium* oocysts. Even for a settling velocity of O(10^{-6}) ms^{-1}, as reported for *Giardia lambia* cysts (Dai and Boll 2006), turbulence intensities (indicated by K_z) in the SML of Lake Tahoe can keep these pathogens in suspension over an extended period of time. Vertical eddy diffusivity K_z at the intake was estimated to be of O(10^{-4}) m^{2}s^{-1} to O(10^{-2})m^{2}s^{-1} in the epilimnion and, thus, 2-4 orders of magnitude larger than the molecular diffusivity (Fig.6). The back-trajectories of those particles originating from near-shore areas <2m depth and withdrawn at the intake reveals transport patterns with respect to the vertical particle position (VPP): (i) the VPP changes frequently between the surface and the bottom in the shallow near-shore beach regions and (ii) the VPP increases progressively until it reaches the depth of the intake (Fig.7). Note that the mean vertical pathogen excursion shown in Fig.6 does not reveal the frequent changes in the VPP. In general, variations of the VPP were restricted to the SML layer and spatially separated from the strongly stratified metalimnion where turbulence is greatly reduced. Consequently, the deepening of the SML caused the pathogens to be transported to greater depth and eventually to the depth of the intake initially located below the SML (Fig.5e). Deepening of the SML occurred in response to enhanced vertical mixing induced by convective cooling and wind shear on a daily basis, thus, increasing the depth to which pathogens were dispersed. The vertical position of a given particle within the water column, in turn, determines the pathogen's survival and inactivation due to temperature and light.
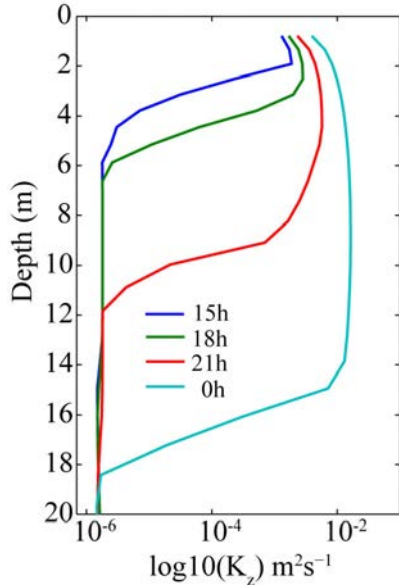
Figure 6. Vertical eddy diffusivity profiles at day 209 15h (blue), 18h (green), 21h (red) and day 210 0h (cyan).
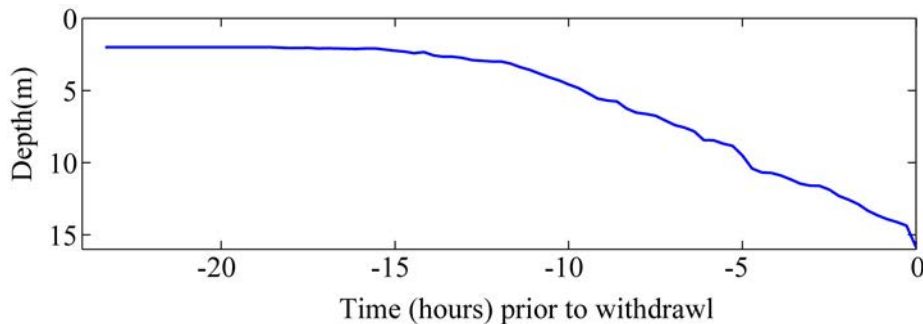
Figure 7. Mean pathogen vertical excursion.

2.3.4 Pathogen inactivation

The oocysts of *Cryptosporidium* are highly sensitive to solar radiation resulting in high light inactivation rates in the very clear waters and high UV flux typical at Lake Tahoe. About 61% of those individuals that originated from shallow beach areas were inactivated due to solar radiation, while temperature inactivation occurred for less than 1% of individuals. The damaging effects of light, especially ultraviolet radiation (UVR), on DNA and the consequences for health and survival of organisms are well known (Sinha and Häder 2002, Häder and Sinha 2005). The effect of radiation on the pathogen infectivity became evident by comparing the number of active (infectious) and inactive pathogens withdrawn during the morning hours (Fig.5d). During the night, 95% of the pathogens withdrawn were infectious, as they travelled in absence of solar radiation during a large part of their trajectory. Although the probability of viable pathogens reaching the intake was highest during the morning hours, it was during the night time when almost all pathogens that reached the intake were infectious.

Given incident short wave radiation values between 1 and 10^3 Wm^{-2}, typical for Lake Tahoe, a light attenuation coefficient k_{UV} of 0.15m^{-1} and a 4-log inactivation dose ID_{99} of 10^3 Jm^{-2}, the time needed to inactivate 99.99% of pathogens ranges from O(1)min-O(1)d at 0.5m depth (Fig.8a). At 16m depth, in contrast, inactivation time scale are one order of magnitude higher, ranging from O(10)min-O(10)d. The different inactivation time scale between 0.5m and 16m depth explain how pathogens could reach the intake during the early morning hours without being inactivated. Once the pathogens have reached a depth where UVR is significantly attenuated, they may continue travelling in spite of the increasing solar radiation reaching the free surface. The predicted time scales are in accordance with Connelly et al. (2007) who found that *Cryptosporidium* is inactivated by >99.99% during 10h of light exposure during a mid-summer day at temperatures comparable to those found at Lake Tahoe (10°-20°C). However, inactivation rates depend on the critical light dose for inactivation ID_{99}. For example, for a critical value of O(10^2) Jm^{-2}, and thus one order of magnitude smaller than the one used in the present study, 79% of the pathogens released would be inactive before reaching deeper waters and, thus, potential water intakes. For a critical value ID_{99} of 10^2 Jm^{-2} (short wave radiation of 1-10^3 Wm^{-2}, k_{UV}=0.15m^{-1}), inactivation time scales would range from O(10)s to O(1)h at 0.5m depth. The predicted scales indicate that pathogens released in shallow water, where they are exposed to high solar radiation intensities, are inactivated within <O(1)d. The inactivation of pathogens is likely to occur within short periods of time as the hours of maximal bathing activity coincide with hours of maximal solar radiation (late morning until early evening). Consequently, the light dose received due to exposure to UVR would have to be low in order for pathogens to be infective when being withdrawn at the intake. Low light (UVR) doses can result from (i) short transport time scales due to short transport distance or high current velocities, and (ii) transport at times or depths of low light intensity.
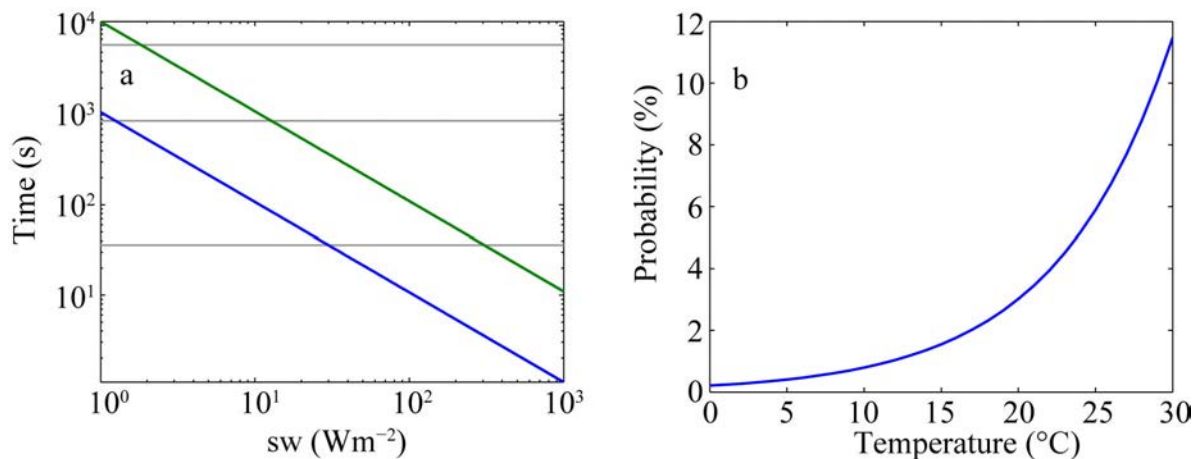
Figure 8.Probability of Cryptosporidium inactivation. Time scale for inactivation due to solar radiation (a) and probability of inactivation due to water temperature following the inactivation rate proposed by Walker and Stedinger (1999) (b). Gray bars in (a) mark 1h, 1d, and 1 week for reference.

Solar radiation is the dominant abiotic agent for pathogen inactivation. At Lake Tahoe, almost 40% of the pathogens withdrawn were predicted to be inactivated due to solar radiation while losses due to temperature were close to zero. The relatively strong effect solar radiation on pathogen inactivation in this large alpine lake might result from high intensities of solar radiation

Flow Modeling and Pathogens
PO # S004422

and high clarity (i.e. low light attenuation with depth), but moderate water temperatures compared to lakes at low altitude and similar latitude. Nonetheless, even for an extreme case of a tropic lake of high turbidity (high light attenuation) and a mean surface temperature of 30°C, we would expect a daily pathogen inactivation due to temperature of ~10% (Fig.8b), while the time scale for a 99.99% inactivation due to light at 0.5m depth would be ~7.5min, assuming a ID_{99} of 10^3 Jm^{-2}, an attenuation coefficient k_{UV} of 3.0m^{-1}, and an incident short wave radiation of 10^3 Wm^{-2}. The high sensitivity of *Cryptosporidium* to radiation is beneficial for the purpose of water disinfection. Low wavelength UVR (typically between 200 and 280 nm) is increasingly applied for disinfection during drinking water treatment (Betancourt and Rose 2004, USEPA 2006, Monis et al. 2014). Solar radiation that the pathogens are exposed to is the principle factor of pathogen inactivation with rates exceeding those of temperature inactivation or losses due to settling. The importance of solar radiation for pathogen inactivation found is in contrast to other studies that did not consider the effect of solar radiation on pathogen infectivity (Anderson et al. 1998, Stewart et al. 2002) or those that considered settling to significantly reduce oocyst concentrations in the water column (Medema et al. 1998, Hawkins et al. 2000). The finding that solar radiation reduces the number of viable pathogens entering drinking water intakes through pathogen inactivation is in agreement with Hipsey et al. (2004). Both pathogen inactivation rates and time scales depend on the specific light parameters (light attenuation coefficient k_{UV} and critical inactivation dose ID_{99}) used, representing the light conditions of a particular lake or lake region. Light attenuation coefficients are typically determined from off-shore Secchi disk measurements (Swift 2004, Rose et al. 2009). However, near-shore (littoral) waters are known to be exposed to higher amount of organic matter (imported from rivers and terrestrial ecosystems) and, thus, are of lower clarity (Swift et al. 2006, Rose et al. 2009). Therefore, off-shore light attenuation coefficients, as have been used here, may overestimate the UV-radiation dose received by pathogens originating from shallow beach areas and, thus, underestimate the risk of pathogen contamination. This effect has not been taken into account into the modeling, primarily because the present understanding of Lake Tahoe's nearshore transparency does not allow for quantification of UV attenuation.

2.4 Conclusions

The risk of pathogens entering drinking water intakes is low (0.02%), but is not totally absent. The risk of pathogens entering water intakes is tightly linked to the stability of the water column, in particular, to the depth of the surface mixed layer. During early and mid-summer, intakes located below the SML are protected by the metalimnion. However, as the summer proceeds, water temperatures increase and the SML deepens, those intakes, if they are not below the summer SML depth, are likely to be exposed to surface water potentially containing human water-borne pathogens. Further, daily fluctuation of the thermocline and the diurnal mixed layer, due to convective mixing at night have been shown to affect the risk of pathogen withdrawal. Thus, the vertical position of the intake in relationship to the expected depth of the thermocline, its seasonal and daily variations, influences the risk of viable pathogens being withdrawn. An obvious outcome of this observation is that to absolutely minimize the risk of human pathogens from body contact recreation being entrained, drinking water intakes should be located at a depth below the oscillation maximum of the summer SML depth. Such considerations would also need to take into account likely lake levels in the face of extreme drought events, during which the intake is closer to the water surface. While distance from a swimming beach would obviously reduce the risk of pathogen entrainment because of UV de-activation, the fact that once the

pathogens are sufficiently deep they tend not to return to the surface, and hence may have very long lifetimes.

Knowledge about daily variation of risk of pathogen withdrawal may help to schedule the times of water withdrawal. High risk was observed to occur during the night with peak intensities in the early morning, as pathogens travel in the dark, protected from harmful solar radiation, and remain infectious when reaching the intake. In contrast, during the daytime, pathogens are inactivated rapidly by solar radiation before reaching the intake and water withdrawal appears to be safe. Thus, water companies could alternate between water withdrawal, during times of near-zero risk, and no withdrawal during times of elevated risk. Special care should be taken at the weekends and holidays when beach visitor density is increased and hours of beach activity may be extended. Also period of strong wind forcing and, thus, strong current velocities may contain a potential risk of pathogens entering water intakes as transport times and exposure times to solar radiation decrease.

Increased light attenuation at the near-shore, where pathogens are released, reduces the light intensities to which pathogens are exposed and increases the risk of pathogen contamination at water intakes. If the light attenuation in the shallow near-shore is unknown or cannot be determined with certainty, using a higher critical light dose for pathogen inactivation may help to prevent underestimating the contamination risk, considering worst case conditions. The high sensitivity of pathogens to solar radiation stresses the importance of water clarity. In clear lakes and reservoirs, solar radiation acts as a mechanism of natural water disinfection. Therefore, water clarity helps to improve water quality and, thus, its maintenance should be of high priority in lake and reservoir management, especially in drinking water sources.

2.5 References

Acosta, M.C., Anguita, M., Rueda, F:J. and F.J. Fernández-Baldomero (2010) Parallel Implementation of a Semi-Implicit 3-D Lake Hydrodynamic Model. Proc. of the 2010 Int. Conf. on Comp. and Math. Methods in Science and Eng. (CMMSE) IV: 1026-1037. gsii.usal.es/~CMMSE/images/stories/congreso/volumen2_10.pdf.

Anderson, M.A. (2008) Lake Tahoe Source Water Protection Risk Assessment. Black & Veatch No.41717.

Antenucci, J.P., Brookes, J.D. and M.R. Hipsey (2005) A simple model for determining pathogen transport and dilution through lakes and reservoirs. J. Am. Water Works Assoc. 2005, 97, 86-93.

Barnes, S.L. 1964. A Technique for Maximizing Details in Numerical Weather Map Analysis. J. Appl. Meteorol. 3: 396-409.

Bitton, G. (1994) Wastewater Microbiology. John Wideley and Sons, Inc., New York.

Brookes, J.D. Davies, C., Hipsey, M.R. and J.P. Antenucci (2004b) Association of Cryptosporidium with Bovine Faecel Particles and Implications for Risk Reduction by Settling within Water Supply Reservoirs. Journal of Water and Health 4, 87-98.

Brookes, J.D., Hipsey, M.R., Burch, M.D., Regel, R.H., Linden, L.G., Ferguson, C.M. and J.P. Antenucci (2005) Relative Value of Surrogate Indicators for the Detecting Pathogens in Lakes and Reservoirs. Environ. Sci. Technol. 39, 8614-8621.

Craik, S.A., Weldon, D., Finch, G.R., Bolton, J.R. and M. Belosevic (2001) Inactivation of Cryptosporidium parvum oocysts using medium- and low-pressure ultraviolet radiation. Water Research 35: 1387-1398.

Dai, X. and J. Boll (2003) Evaluation of attachment of Cryptosporidium parvum and Giardia lamblia to soil particles. Journal of Environmental Qual. 32: 296-304.

Dai, X. and J. Boll (2006) Settling velocity of Cryptosporidium parvum and Giardia lamblia. Water Research 40: 1321-1325. Doi:10.1016/j.watres.2006.01.027

Feachem, R.G., Bradley, D.J., Garelick, H. and D.D. Mara (1983) Sanitation and Disease. John Wiley and Sons, Inc., New York.

Farthing, M.J.G. (2000) Clinical aspects of human cryptosporidiosis. In Cryptosporidiosis and microsporidiosis (Eds Petry, F. and B. Karger) Contrib Microbiol. 6, 50-74.

Fischer, H. B., E. J. List, R. C. Y. Koh, J. Imberger and N. H. Brooks (1979) Mixing in Inland and Coastal Water. Academic Press, New York.

Gardner, J.V., L.A. Mayer and J.E. Hughes Clark. 1998. Cruise Report, RV Inland Surveyor Cruise IS-98: The bathymetry of Lake Tahoe, California-Nevada: U.S. Geological Survey Open-File Report 98-509, 28p. <http://blt.wr.usgs.gov>

Haeder, D.-P. and R.P. Sinha (2005) Solar ultraviolet radiation-induced DNA damage in aquatic organisms: potential environmental impact. Mutation Research 571: 221-233.

Han, Y.-J., Holsen, T.M., Hopke, P.K. and S.-M. Yi (2005) Comparison between Back-Trajectory Based Modeling and Lagrangian Backward Dispersion Modeling for Locating Sources of Reactive Gaseous Mercury. Environ. Sci. Technol. 39, 1715-1723.

Hawkins, P.R., Swanson, P., Warnecke, M., Shanker, S.R. and C. Nicholson (2000) Understanding the Fate of Cryptosporidium and Giardia in Storage reservoirs: A Legacy of Sydney's Water Contamination Incident. Aqua 49(6): 289-306.

Hipsey, M.R., Antenucci, J., Brookes, J.D., Burch, M.D., Regel, R.H. and L. Linden (2004) A three dimensional model of Cryptosporidium dynamics in lakes and reservoirs: a new tool for risk management. Intl. J. River Basin Management 2(3), 181-197.

Hipsey, M.R. and J.D. Brookes (2013) Pathogen Management in Surface Waters: Practical Considerations for Reducing Health Risk. In: A.Rodríguez-Morales, Current Topics in Public Health, InTech, DOI: 10.5772/55367.

Hoyer, A.B., Wittmann, M.E., Chandra, S., Schladow, S.G. and F.J. Rueda (2014a) A 3D individual-based aquatic transport model for the assessment of the potential dispersal of planktonic larvae of an invasive bivalve. Journal of Environmental Management.

Hoyer, A.B., Schladow, S.G. and F.J. Rueda (2014b) Local Dispersion of invasive bi-valve Species by Wind-driven Lake Currents. Submitted to Limnology and Oceanography: Fluids and Environments.

Jakubowski, W. (1984) Detection of Giardia cysts in drinking water: State of the art. In: Giardia and Giardiasis, Biology, Pathogenesis and Epidemology, pp. 263-285. Plenum Press, New York.

Jenkins, M., Anguish, L., Bowman, D., Walker, M. and W. Ghiorse (1997) Assessment of a dye permeability assay for the determination of inactivation rates of Cryptosporidium oocysts. Appl. and Envir. Microbiology 63(10), 3844-3850.

Largier, J. (2003) Considerations in estimating larval dispersal distances from oceanographic data. Ecological Appl. 13(1), S71-S89.

Flow Modeling and Pathogens
PO # S004422

Liu, L., Phanikumar, M.S., Molloy, S.L., Whitman, R.L., Shively, D.A., Nevers, M.B., Schwab, D.J. and J.B. Rose (2006) Modling the Transport and Inactivation of E. coli and Enterococci in the Near-Shore Region of Lake Michigan. Environ. Sci. Technol. 40, 5022-5028.

Medema, G.J., Schets, F.M., Teunis, P.F.M. and A.H. Havelaar (1998) Sedimentation of Free and Attached Cryptosporidium Oocysts and Giaria Cysts in Water. Applied and Environmental Microbiology 64(11), 4460-4466.

Medema, G. (2013) Microbial Risk Assessment of Pathogens in Water. In: Environmental Toxicology, pp 361-401.

Monis, P., King, B. and A. Keegan (2014) Removal and Inactivation of Cryptosporidium from Water. In: S.M. Cacciò and G. Widmer. Cryptosporidium: parasite and disease. Springer, pp.515-552.

Morita, S., Namikoshi, A, Hirata, T, Oguma, K., Katayama, H, Ohgaki, S., Motoyama, N. and M. Fijiwara (2002) Efficacy of UV irradiation in inactivating Cryptosporidium parvum oocysts. Applied and Environmental Microbiology 68, 5387-5393.

Nickols, K., Gaylord, B. and J. Largier (2012) The coastal boundary layer: predictable current structure decreases alongshore transport and alters scales of dispersal. MEPS 464, 17-35.

Ongerth, J.E. and Pecoraro, J.P. (1996) Electrophoretic mobility of Cryptosporidium parvum and Giardia lamblia cysts. Journal of Environmental Engineering 122(3), 228-231.

Rao, Y.R. and D.J. Schwab (2007) Transport and Mixing Between the Coastal and Offshore Waters in the Great Lakes: a Review. J. Great Lakes Res. 33: 202-218.

Reynolds, C.S. (1984) The Ecology of Freshwater Phytoplankton. Cambridge University Press, Cambridge.

Robertson, L.J., Smith, H.V. and C.A. Paton (1995) Occurrence of Giardia and Cryptosporidium ooystes in sewage effluent in six sewage treatment plants in Scotland and the prevalence of cryptosporiosis and giardiasis diagnosed in the communities served by those plants. In: Protozoan Parasites and Water, eds: W.B. Betts, D. Casemore, C. Fricker, H. Smith and J. Watkins, pp.47-49. The Royal Society of Chemistry, Cambridge.

Rueda, F.J. and S.G. Schladow. 2002. Quantitative comparison of models for barotropic response of homogenous basins. J. Hydraul. Eng. 128: 201-213.

Rueda, F.J. and S.G. Schladow. 2003. Dynamics of Large Polymictic Lake II: Numerical Simulations. J. Hydraul. Eng. 129: 92-101.

Rueda, F.J. and E.A. Cowen. 2005. Residence Time of a Freshwater Embayment Connected to a Large Lake. Limnol. Oceanogr. 50: 1638-1653.

Rueda, F.J., S.G. Schladow and S.O. Pálmarsson. 2003. Basin-scale internal wave dynamics during a winter cooling period in a large lake. J. Geophys. Res. 108: 3097, doi:10.1029/2001JC000942.

Rueda, F.J., S.G. Schladow and J.F. Clark. 2008. Mechanisms of contaminant transport in a multi-basin lake. Ecol. Appl. 18: A72-A88.

Sinha, R.P. and D.-P. Haeder (2002) UV-induced DNA damage and repair: a review. Photochem. Photobiol. Sci. 1, 225-236.

Smith, P.E. (2006) A Semi-implicit, Three-dimensional Model for Estuarine Circulation. Open-File Report 2006-1004. U.S. Department of the Interior, U.S. Geological Survey.

Sterk, A., Schijven, J.F., de Nijs, T. and A.M. De Roda Husman (2013) Direct and indirect effects of climate change on the risk of infection by water-transmitted pathogens. Environmental Science and Technology.

Stewart, M.H., Yates, M.V. Anderson, M.A., Gerba, C.P., Rose, J.B., De Leon, R. and R.L. Wolfe (2002) Predicted public health consequences of body-contact recreation on a potable water reserovir. Jour. AWWA 94, 84-97.

Swift, T.J. 2004. The aquatic optics of Lake Tahoe CA-NV. Thesis. University of California, Davis, California, USA.

Swift, T.J., Perez-Losada, J. Schladow, S.G., Reuter, J.E., Jassby, A.D. and C.R. Goldman. 2006. Water clarity modeling in Lake Tahoe: linking suspended matter characteristics to Secchi depth. Aquatic Sciences 68, 1-15.

Walker, F.R. and J.R. Stedinger (1999) Fate and Transport Model of Cryptosporidium. Journal of Environmental Engineering 125(4), 325-333.

Williamson, C.E., Dodds, W., Kratz, T.K. and M.A. Palmer (2008) Lakes and streams as sentinels of environmental change in terrestrial and atmospheric processes. Front. Ecol. Environ. 6(5), 247-254.

Wu, J., Rees, P, Storrer, S., Alderisio, K. and S. Dorner (2009) Fate and Transport Modeling of Potential Pathogens: The Contribution From Sediments. Journal of the American Water Resources Association (JAWRA) 45(1), 35-44. Doi:10.111/j.1752-1688.2008.00287.x

Yates, M.V. et al. (1997) The Impact of Body-contact Recreation in the Eastside Reservoir Project on (1) Pathogen Risk to Consumers and Recreators and (2) MTBE Contamination. Final report submitted to MMDSC.

3. Pathogen Concentrations and Consumer Health Risks Resulting from Body-Contact Recreation Near Water Intakes of Kingsbury General Improvement District and Edgewood Water Company with LT2-Compliant Treatment

3.1 Introduction

Swimming and other recreational activities that involve direct human contact with water have been found to negatively impact water quality in some settings (Rose *et al.*, 1987; Calderon *et al.*, 1991; Kramer *et al.*, 1996; Sunderland et al., 2007). Because of difficulties and costs associated with sampling and detection, concentrations of pathogens in recreator-impacted waters and the associated health risks to consumers and recreators remain poorly understood. As a result, numerical simulations have been used to estimate pathogen concentrations in source drinking water reservoirs, including a recent risk assessment for selected intakes on Lake Tahoe (Black and Veatch, 2008).

In that study, Monte Carlo (MC) techniques were incorporated into a finite segment-based pathogen transport model to predict pathogen concentrations due to body-contact recreation near the Burnt Cedar intake (Incline Village General Improvement District, IVGID), the McKinney/Quail intake operated by the Tahoe City Public Utilities District (TCPUD), and the Kingsbury Grade intake (Kingsbury General Improvement District, KGID) (Black & Veatch, 2008). That study focused on *Cryptosporidium*, due to its low infective dose, persistence in the environment, and resistance to conventional disinfection. The modeling approach adopted in that risk assessment required information about the distribution and intensity of recreational use, prevalence of cryptosporidiosis within the community (especially asymptomatic infections), fecal shedding rate, loss processes within the water column, including inactivation and settling, advective and dispersive transport processes, location of intake, and effectiveness of water treatment/disinfection.

The Burnt Cedar intake was found to have the highest level of adjacent recreational use and lowest treatment efficiency of the 3 intakes evaluated. Model simulations yielded a median annual *Cryptosporidium* concentration of 0.0023 oocysts/100 L (Black and Veatch, 2008). The ozone treatment plant there achieved only about 55% removal of oocysts during the summer. As a result, risk calculations yielded a median annual risk level of 0.28 infections per 10,000 consumers per year and further indicated a 7.6% probability of exceeding the USEPA target risk level of 1 infection/10,000 consumers/yr (Black and Veatch, 2008). High recreational use and low treatment efficacy at the Kingsbury Grade intake also resulted in a high predicted median annual concentration (0.0018 oocysts/100 L) and a 4.9% probability of exceeding the USEPA target risk level. A much lower predicted median concentration and exceedance probability were found for the McKinney/Quail intake (0.00023 oocysts/100 L and <0.02%, respectively) due to more effective filtration-based treatment and lower intensity of recreational use (Black and Veatch, 2008).

Simulations further indicated that the risk of infection due to *Cryptosporidium* to water consumers on the Burnt Cedar and Kingsbury Grade systems would be substantively reduced through adoption of more effective treatment technologies. For example, a 2-log (99%) removal

at the treatment plants, e.g., using UV-disinfection, was predicted to reduce the probability of exceeding the USEPA risk target to <0.1% for these intakes.

The Long-Term 2 Enhanced Surface Water Treatment Rule (LT2 rule) was specifically developed by the USEPA to provide additional consumer protection against *Cryptosporidium* and other disease-causing microorganisms in drinking water drawn from surface water or ground water under the direct influence of surface water, especially unfiltered systems and filtered systems with high levels of *Cryptosporidium* in their source waters. The LT2 rule requires unfiltered systems to meet treatment technique requirements for *Cryptosporidium* no later than October 1, 2014. Incline Village General Improvement District has upgraded the Burnt Cedar water treatment plant to include UV treatment, while KGID is completing construction of a new ozone/UV water treatment plant. These improvements are thus expected to markedly improve the quality, safety and reliability of drinking water for their customers.

At the same time, however, two significant development projects are planned near/within the shorezone adjacent to the KGID and Edgewood Water Company's intakes: the Edgewood Lodge and Golf Course Improvement Project with new public beach and relocated-expanded pier, and the Beach Club and associated beach on Lake Tahoe. This study was undertaken to assess the cumulative impacts on finished drinking water quality and consumer public health due to increased recreational use near the KGID and Edgewood intakes and treatment plant upgrades required by LT2.

3.2 Approach

The consumer risk levels resulting from body-contact recreation near the Kingsbury Grade and Edgewood intakes were calculated using a pathogen fate model coupled with calculations describing *Cryptosporidium* removal at their corresponding treatment plants and application of a dose-response model following the previous risk assessment (Black & Veatch, 2008). A refined finite difference model was constructed to predict *Cryptosporidium* transport and fate, with oocysts shed by body-contact recreators subject to advective and dispersive transport, as well as loss due to inactivation and settling.

As previously described (Black and Veatch, 2008), this approach involves dividing the lake or embayment into a series of smaller segments or volume elements (Thomann and Mueller, 1987). For each segment, the change in the number of pathogens in any segment i (N_i) under conditions of varying volume as a function of time (t) is given by:

$$\frac{dN_i}{dt} = \frac{dV_i C_i}{dt} = V_i \frac{dC_i}{dt} + C_i \frac{dV_i}{dt} \tag{3.1}$$

where V_i is the volume of segment i (m^3) and C_i is the pathogen concentration in segment i (pathogens m^{-3}). The first term on the right-hand side of eq 3.1 can be rewritten as (Anderson et al., 1998; Black and Veatch, 2008):

$$V_i \frac{dC_i}{dt} = \sum_n (Q_{ij} C_j - Q_{ij} C_i) + \sum_j E_{ij}^* (C_j - C_i) + \sum_{R_i} IM_f P + \sum_{R_i} IFM_{AFR} P$$
$$- kC_i V_i - \upsilon_i A_i C_i \tag{3.2}$$

Flow Modeling and Pathogens
PO # S004422

where Q_{ij} refers to flow between segments i and j (m^3 d^{-1}), E^* is a dispersion coefficient describing dispersive flux between neighboring segments i and j (m^2 d^{-1}), I is the age-weighted prevalence rate, M_f is the mass of fecal material shed (g), P is the pathogen content of the fecal material (pathogens g^{-1}), F is the AFR frequency, M_{AFR} is the mass of AFR (g), k is the inactivation rate constant for the pathogen (d^{-1}), v is the settling velocity of the pathogen (m d^{-1}), and A is the segment cross-sectional area (m^2). One notes that inputs from fecal shedding and AFRs are summed over R_i, the number of recreators on a segment i.

Since the volume of Lake Tahoe and smaller embayments vary only modestly over a year, approximate steady-state with respect to volume was assumed (i.e., $dV_i/dt=0$), so the 2nd term on the right hand side of eq 3.1 drops out, and eq 3.2 forms the basis for the model. The finite-segment model (eq 3.2) requires basic physical information about the segment volumes, cross-sectional areas, advective flows and dispersive transport into and out of the segments, as well as infection state, recreational use, and loss processes serving to remove pathogens from the water column.

Due to both the sensitivity of the model to a number of parameters as well as the large uncertainty in parameter estimates within the published literature, a probabilistic modeling approach has previously been used (Yates et al., 1997; Anderson et al., 1998; Black & Veatch, 2008) and was adopted in this study as well. Monte Carlo techniques are used to both describe pathogen inputs and implement a formal uncertainty analysis. The uncertainty analysis involves a large number of simulations (5000) wherein model parameter values describing the pathogen input, transport and loss are randomly drawn from within appropriate distributions. Thus, excluding some basic elements resulting from model segmentation (e.g., segment volumes, cross-sectional areas), a range in model parameters are evaluated in the analysis and the impacts on predicted water quality are presented using probabilistic descriptions.

3.3 Model
3.3.1 Grid
The southeast corner of Lake Tahoe near the KGID and Edgewood Water Company intakes, just north of the Nevada line, was divided into 3200 lateral segments (2347 wet segments) on an orthogonal 50 m x 50 m grid. The grid was overlain on bathymetry derived from the digital elevation map (DEM) data developed by the USGS for Lake Tahoe (http://tahoe.usgs.gov/bath.html) (Fig. 3.1a).
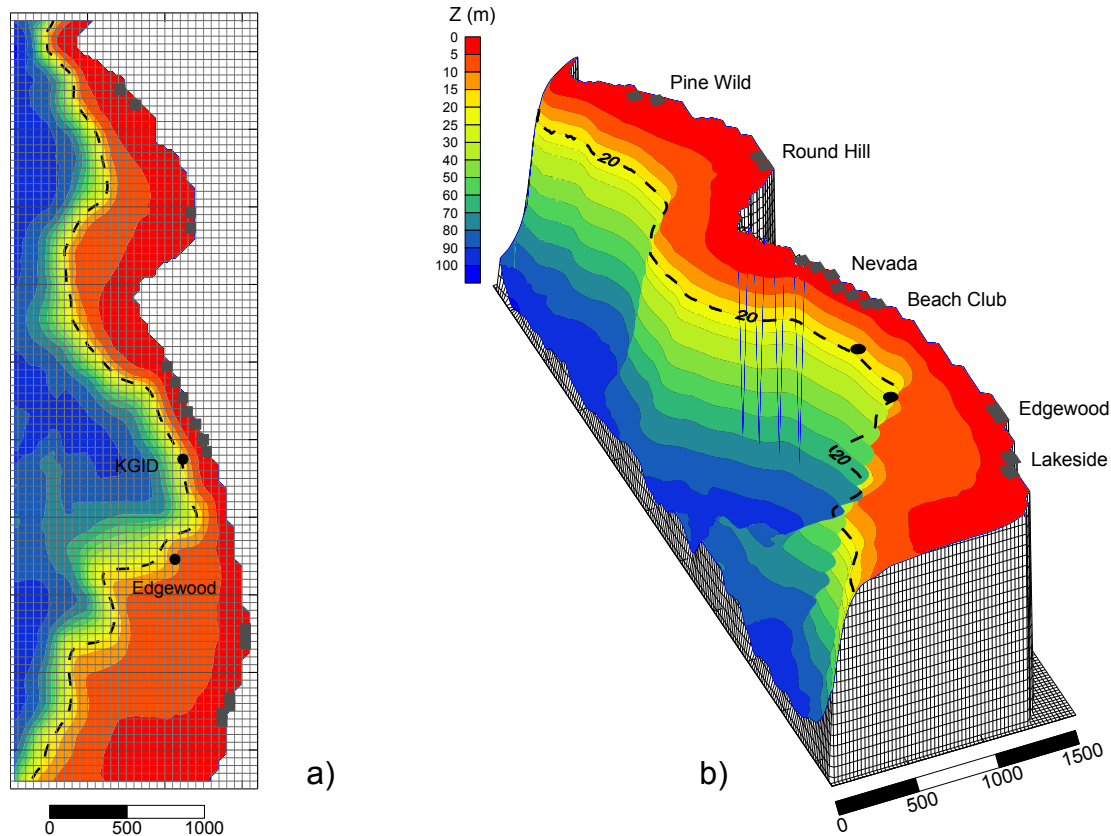
Fig. 3.1. Bathymetry and segmentation for the numerical model for the Kingsbury Grade and Edgewood water intakes. a) bathymetry represented as contour plot with computational grid overlain; b) bathymetry represented as wireframe with beaches identified.

Temperature profiles for the lake indicate the epilimnion extends down about 20 m during the summer, while a relatively well-mixed water column extending to 100-200 m depth is present during the winter. Summer stratification is typically present June-November (duration of stratification about 188 days) (TERC, 2013). 3-D simulations of the hydrodynamics and larval transport in Marla Bay and areas adjacent to the intakes indicate a mixed layer depth of approximately 20 m (Hoyer et al., 2014). For these simulations, the surface mixed layer was taken as the full depth within the computation domain (Fig. 3.1) through May, reduced to 20 m during the summer-fall (Fig. 3.1, dashed line), and mixed again in December. Segment volumes (V_i) were calculated from bathymetric and grid data and ranged from $311 - 102,551$ m^3 (fully-mixed) with a median volume of 58,000 m^3. Segment volumes >50,000 m^3 were reduced to 50,000 m^3 (50 m x 50 m x 20 m) to represent the mixed layer during summer stratification. The 100 segments adjacent to the shoreline (and beaches) had an average volume of 2,836 m^3 and average depth of 1.2 m.

3.3.2 Transport Processes

Water movement across Lake Tahoe can vary greatly over space and time. In the earlier risk assessment (Black and Veatch, 2008), circulation near the KGID intake was estimated from surface drifters and thermal satellite imagery (Steissberg et al., 2005) and basin-scale simulations of Reuda et al. (2003). As described in chapter 2 of this report, a much finer computational grid

Flow Modeling and Pathogens
PO # S004422

was used to provide more accurate representations of the wind-driven circulation near the KGID and Edgewood intakes. As in the previous risk assessment (Black & Veatch, 2008), it was necessary to reduce the fine sub-daily features of advective and convective transport to daily mixed-depth averaged values to facilitate the Monte Carlo simulations conducted herein. Average daily values for the east and north components of the velocity vector for currents near the intakes were transformed into vector velocity magnitude and direction using standard trigonometric relationships.

Water movement was strongly directional near the KGID intake, with depth-averaged advective velocities (Fig. 3.2) oriented alongshore (Fig. 3.1). Depth-averaged velocities within the epilimnion/mixed layer at the intake were typically 1-2 cm/s, although depth-averaged velocities exceeding 4 cm/s were also periodically present; strongest flow was to the NNW, although weaker currents directed to the SSE were also present (Fig. 3.2a). Water currents in the mixed layer near the Edgewood intake were more frequently directed toward shore (~70° relative to N) but slow moving currents to the S-SSW were also common (Fig. 3.2b). As noted in chapter 2, surface velocities were often much higher than depth-averaged values depicted here.
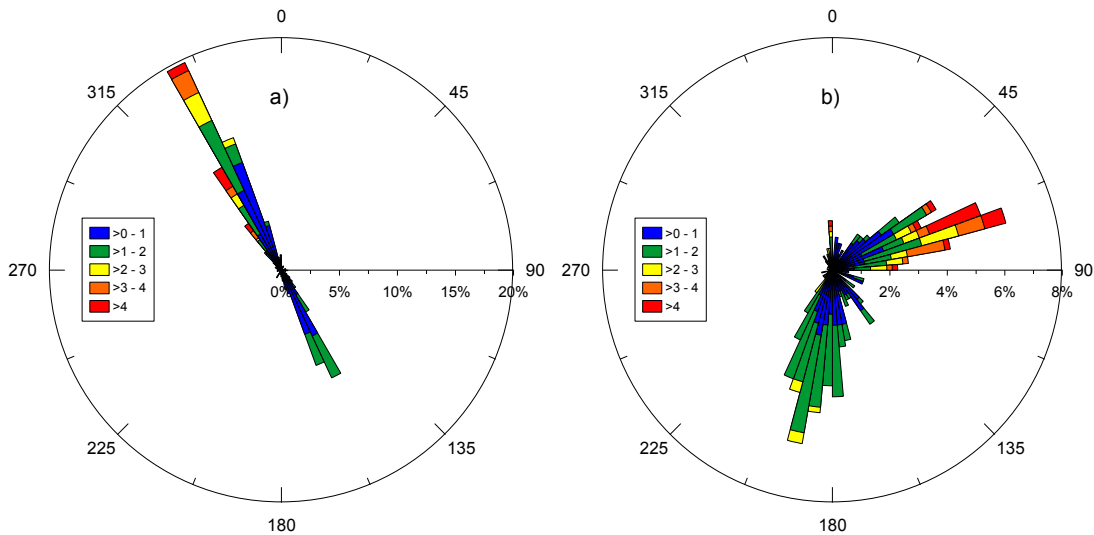

Fig. 3.2. Depth-averaged mixed-layer current velocities (cm/s) near a) KGID and b) Edgewood intakes.

Dispersion due to turbulent diffusion between neighboring segments is also an important transport process in lakes (Thomann and Mueller, 1987; Martin and McCutcheon, 1999; Chapra, 1997). Horizontal turbulent diffusion coefficients (E_{ij}) have been shown to increase with length scale, with values of approximately 10^4-10^5 m^2/d reported for Lake Ontario and the ocean at 1-10 km length scales (Chapra, 1997). E_{ij} was allowed to vary log-uniformly from 10^4-10^5 m^2/d. The bulk exchange coefficient E^*_{ij} was calculated as:

$$E^*_{ij} = \frac{E_{ij} A_{ij}}{\Delta X_{ij}}$$ (3.3)

where E_{ij} is the effective (horizontal) dispersion coefficient (m^2/d), A_{ij} is the interfacial area between segments i and j (m^2), and ΔX_{ij} is the distance from the centroid of i to j (m) (Thomann and Mueller, 1987).

3.3.3. Recreational Use and Pathogen Inputs

Pathogen concentrations at the KGID and Edgewood intakes are directly related to the magnitude and location of inputs. As in the previous risk assessment (Black and Veatch, 2008), inputs were restricted to swimmers and other individuals participating in body-contact recreation near shore. Sewage discharge from boats and other sources have been explicitly excluded in these simulations. Moreover, while jet skiers and waterskiers can be potential sources of pathogens, they were also excluded from this analysis due to the frequent use of wetsuits by such individuals on the lake, combined with their unknown but low use rates relative to swimmers and other body-contact recreators at the beaches.

Body-contact recreational use near the Kingsbury Grade and Edgewood intakes was estimated from July 2nd-4th, 2006 beach survey results (Black and Veatch, 2008) and projected use at the new beaches at the Edgewood Lodge/Resort and Beach Club developments. A large number of locations exist near the intakes where body-contact recreation occurs (Fig. 3.1b). The analysis of recreational use conducted as part of the prior risk assessment assumed an average of 1440±290 individuals participated in body-contact recreation at nearby beaches during summer weekend/holiday use, with lower weekday use, on the order of 206±41 body-contact recreators per day. Body-contact recreational use at the new beaches was estimated based upon length of the new Edgewood Lodge/Resort and Beach Club beaches (approximately 560 and 220 ft, respectively), number of units associated with the developments (about 200 and 140, respectively), beach access and facilities. The intensity of body-contact use at the popular Nevada Beach over the summer recreational season provided one way to estimate predicted use rates; specifically, intensity was taken as total body-contact recreational use at Nevada Beach (26,104/yr) (Black & Veatch, 2008) divided by length of shoreline (approximately 3000 ft) for a use intensity of about 9/ft/yr. This use intensity, when multiplied by the lengths of the Edgewood Lodge/Resort and Beach Club beaches, translates to about 5,040 and 1,980 body-contact recreators each summer.

Body-contact use was separately estimated from the number of units in each of the proposed developments assuming double-occupancy with all units filled and one-half of occupants participating in body-contact recreation each summer weekend. Using this approach, approximately 200 individuals at the Edgewood Lodge/Resort and 150 individuals at the Beach Club would participate in body-contact recreational use on each of the 32 weekend and holiday days. Use was reduced to about 1/7th for weekdays following Black & Veatch (2008), yielding total summer body contact recreational use of 8,372 and 6,228, respectively. These values were 1.7-3x higher than predicted from Nevada Beach use intensity. These higher levels of use were adopted in model simulations, thus increasing by 25% the average regional body-contact recreational use, with this increase explicitly allocated to the new beach areas (Fig. 3.1b; Fig. 3.3). Extrapolating to the full summer use at all beaches near the intakes (Fig. 3.1b), one estimates the total number of individuals participating in body-contact recreation to increase

Flow Modeling and Pathogens
PO # S004422

from 60,088±12,101 to 74,688±15,041 each summer. Total regional visitation is projected to be approximate of recreational use on predicted annual risk of infection for water consumers is further assessed later in this chapter.
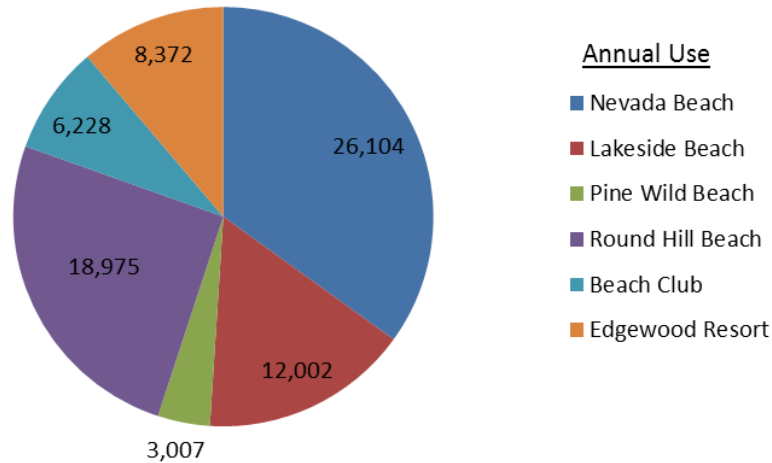

Fig. 3.3. Projected average annual body-contact recreational use (total annual body-contact use projected to be 74,688±15,041)

In addition to the total or daily number of recreators, the location of their swimming and related activities also has a potentially quite important role in their impact on microbial water quality in the raw (and finished) water. The 2006 beach survey results, combined with projected use at Beach Club and Edgewood Lodge/Resort, indicates that 43% of total regional recreational use will occur at Nevada Beach and Beach Club beach in close proximity to the KGID intake (Fig. 3.1, Fig. 3.3). In contrast, Pine Wild Beach has little annual use and is sufficiently removed from the intakes that it presents little risk to intake water quality. This data was used with Monte Carlo techniques to distribute recreators across the main swimming beaches (Fig. 3.3).

The prevalence rate of infection due to *Cryptosporidium* within the recreator community is a model parameter that, along with the number of recreators, plays a central role in defining the total oocyst loading to a recreationally-impacted water body (Yates et al., 1997). Considerable variability exists in the literature about the non-outbreak prevalence rates of cryptosporidiosis, however (*e.g.*, Amin, 2002; Frost et al., 2000; Frost et al., 2001; McDonald et al., 2001; Ungar, 1990; Soave and Weikel, 1990). Results of these studies yielded non-outbreak prevalence rates of 0.8 – 4.2 %, with a mean of 1.6±0.8 %. The prevalence rate for any given simulation was thus drawn from a normal distribution with a standard deviation of 0.8% about this value (Table 3.1).

Table 3.1. Parameters affecting pathogen input and the ranges and distribution used in simulations for Monte Carlo uncertainty analyses.

Parameter	Range	Distribution
Prevalence Rate (%)	1.6 ± 0.8	Normal
Feces shed (g/person)	$0.01 - 1$	Log-uniform
Pathogen content (per g)	$10^5 - 10^7$	Log-uniform
AFR frequency (per 1000)	$0 - 2$	Uniform
Mass of AFR (g/AFR)	$50 - 200$	Uniform

It is necessary to also define the release of fecal material through body-contact, either through shedding or through so-called "accidental fecal releases" (AFRs), as well as the pathogen content of the feces (eq 3.2). Values used in the previous risk assessment (Black and Veatch, 2008) were also used in this study (Table 3.1). Specifically, fecal shedding rates (M_f) of $0.01 - 1$ g/person, AFR frequency (F) of 0-2 AFRs/1000 recreators, and mass of AFR (M_{AFR}) of 50-200 g/AFR were assumed for these calculations.

Since only a small portion of the total number of swimmers will be infected (presumably asymptomatically) with *Cryptosporidium*, it is likely, for example, that only a few recreators during the week, and perhaps just a few dozen during the weekend, will actually serve as sources of oocysts to the lake. Since one does not know *a priori* who is infected and who is not, nor where along the beach they may choose to swim, deterministic modeling is not appropriate. As a result, Monte Carlo (MC) techniques were incorporated into the finite segment model so that the occurrence of infection and AFRs, mass of feces shed, mass of AFR, pathogen content of feces, and location were evaluated for each recreator, and conform only in the ensemble-averaged sense to the population-averaged prevalence rate, AFR frequency, and other statistics (Anderson et al., 1998; Black and Veatch, 2008). For example, given some prevalence rate for the recreator population, MC can be used to test the infection state of each recreator such that the ensemble-averaged infection rate is equivalent to a population average value without specific assumptions about individual recreators. As in the prior risk assessment, MC techniques were also used to define individual recreator shedding characteristics (*e.g.*, fecal shedding rate, pathogen content) that could be expected to differ significantly across a population (Fig. 3.4).

Thus, for each day during the simulation period, the total number of recreators participating in body-contact recreation was determined. Each recreator was then tested for infection by randomly drawing a real number between 0 - 1 and determining whether that number lies within an interval defined by the prevalence rate for the recreator population. If the recreator was found to be non-infected, additional recreators were then tested until all recreators projected to be participating in body-contact recreation that day in the simulation were evaluated. If a particular recreator is infected, then further MC tests were performed to define shedding characteristics. Each infected recreator was tested for fecal shedding rate by using MC to randomly sample the shedding rate from within a log-uniform distribution (Table 3.1). The (infected) recreator was then tested for an AFR in a fashion similar to that used to establish infectivity. If positive, the mass of AFR was randomly assigned from a uniform distribution (50-200 g/AFR), which combined with the mass of fecal material shed through contact with the water, determined the total fecal input from that recreator (Black and Veatch, 2008).
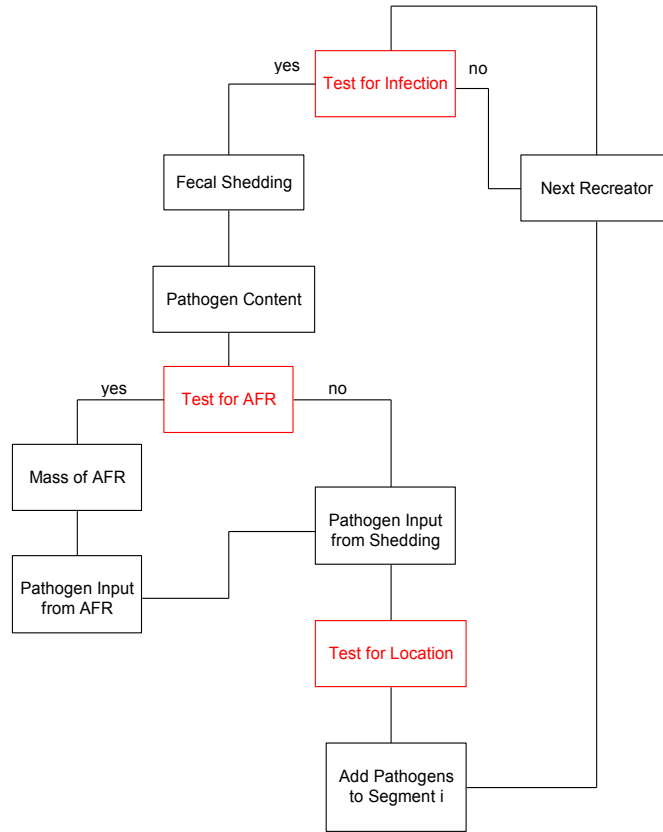
Fig. 3.4. Flowchart describing recreator analysis.

Following assignment of the mass of feces released by an infected individual, the *Cryptosporidium* content of the feces was then determined. The *Cryptosporidium* content of feces was allowed to vary between 10^5-10^7 oocysts/g feces for each of the individual recreators. The pathogen input was taken as the product of the total mass of fecal material released to the water and the pathogen content of the feces. The final step involved placing the recreator at one of the beaches; this was also done using MC, where the placement of the swimmer was determined by drawing a random number between $0 - 1$ and then placing that individual at a location consistent with spatial use patterns (Fig. 3.3).

3.3.4. Loss Processes

Cryptosporidium can be lost from the water column due to inactivation and settling. Walker and Stedinger (1999) developed an empirical temperature-dependent inactivation rate constant, k (d^{-1}) given as:

$$k = 10^{-2.68} \, 10^{0.058 \, T} \qquad (3.4)$$

where T is the temperature in °C. An analysis that includes additional inactivation data yielded a best fit equation with slightly different slope and intercept values (Black and Veatch, 2008):

$$log \ k = -2.34 \pm 0.173 + (0.0415 \pm 0.0094)*T \qquad (3.5)$$

Standard deviations about the slope and intercept values were defined so that uncertainty in inactivation rate constants at any given temperature could also be established; for the model calculations, the slope and intercept terms were randomly drawn from Gaussian distributions about the mean values for these 2 parameters.

Temperature records from the KGID treatment plant (Fig. 3.5) were used in conjunction with eq 3.5 to define the inactivation rate constant over time. Temperature trends were reasonably fit with 3 linear regressions, with temperatures near 6°C in the winter, warming to about 16°C in summer, and then quickly cooling in the fall (Fig. 3.5). The equations describing temperature over time are:

for day <100:	*Temp (°C) =-0.00499*Day+6.58*	*(3.6)*
for day 100-260:	*Temp (°C) = 0.0629*Day – 0.12*	
for day >260:	*Temp (°C) = -0.110*Day+44.81*	

A median natural inactivation rate constant for *Cryptosporidium* of 0.021 d^{-1} in the summer is thus predicted. Following the previous risk assessment (Black and Veatch, 2008), natural UV inactivation was not explicitly included, but is discussed later in this report.
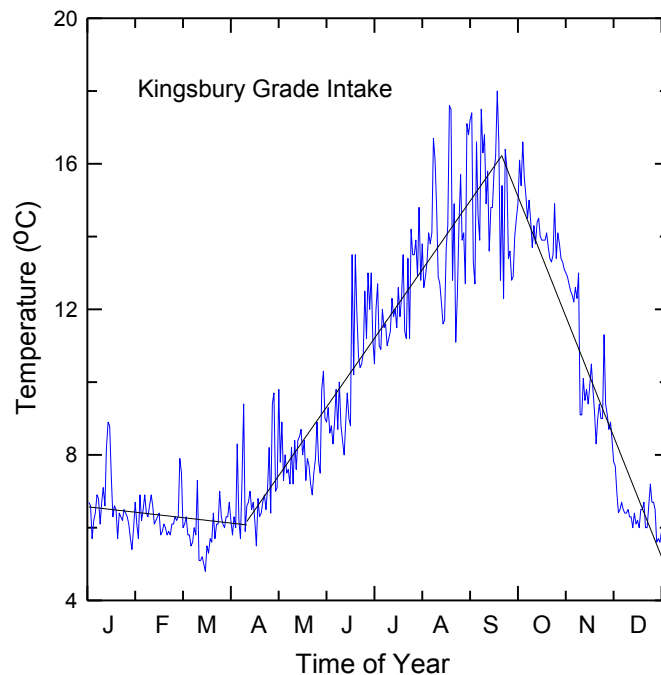

Fig. 3.5 .Water temperature over time recorded for the KGID intake. Dashed line is temperature model-fitted result.

Settling of oocysts is also a potentially important loss process (Medema et al., 1998). Medema et al. (1998) reported experimentally measured settling rates for free oocysts of 0.05

Flow Modeling and Pathogens
PO # S004422

m/d, although the aggregation state of shed fecal material and potential association of oocysts with particles is not known *a priori*. Medema et al. (1998) experimentally demonstrated that settling velocity increased substantially, exceeding 0.5 – 1 m/d, when oocysts were attached to particles in biologically treated sewage effluent, thus suggesting that settling may be an important loss process for shed, particle-associated oocysts in lakes and reservoirs.

Since the aggregation state of oocysts in shed fecal material remains unknown, the settling velocity was treated as a stochastic variable both in the previous study (Black and Veatch, 2008) and in this assessment. The settling velocity was allowed to vary from 0.05 m/d (for free oocysts) to that found in lab and field studies (1.0 m/d) (Medema et al., 1998) following a log-uniform distribution, with a median settling velocity of 0.22 m/d. Additional corrections were made for resuspension due to turbulence resulting from the orbital motion associated with surface waves, as well as bottom currents, consistent with recent studies on Asian clam larval transport (Hoyer et al., 2014). That is, wave action and bottom currents keep particles from settling in shallow near-shore locations; Hoyer et al. (2014) reported frequent resuspension up to depths of 6 m near Marla Bay. In this study, no settling was allowed for the 100 shallow beach segments (i.e., correction factor of 0, resuspension frequency of 100%), while the correction factor was allowed to increase with depth to a value of 0.5 at 10 m depth and no correction was applied at depths greater than 10 m. Thus only at segments >10 m depth did settling rates fully reach the 0.05 - 1.0 m/d range, although as shown in chapter 2, settling is a minor loss process for free oocysts.

3.3.5. Uncertainty Analysis

As indicated above, the model is strongly sensitive to a number of model parameters, including mass of feces shed (M_f), frequency and mass of AFRs (F and M_{AFR}, respectively), pathogen content of feces (P), prevalence or infection rate (I), and inactivation rate (k). Considerable variability exists in the literature for many of these parameters, and in some instances, limited information is available. Accordingly, an uncertainty analysis was conducted in which >5000 simulations were performed using population or global parameter values randomly selected from within defined ranges based upon literature values and expert consensus.

3.4. Removal of *Cryptosporidium* at Treatment Plant

With predictions of the *Cryptosporidium* concentrations across the computational domain, concentrations at the KGID and Edgewood intakes represented concentrations delivered to the treatment plants. The inactivation of *Cryptosporidium* from the raw water at the upgraded KGID and Edgewood ozone-UV treatment plants were then calculated. Oocyst inactivation due to ozone treatment was calculated following Rakness et al. (2005) using the equation:

$$\log (N_0/N) = k_{10,C}CT \qquad (3.7)$$

where N_0 is the intake pathogen concentration, N is the effluent concentration, $k_{10,C}$ is the ozone inactivation rate coefficient for *Cryptosporidium*, and CT is ozone concentration*time. The ozone inactivation rate constant is dependent upon temperature (Temp), following the relation:

$$k_{10,C} = 0.0397*(1.09757)^{Temp} \tag{3.8}$$

Regressions between CT and temperature for KGID were developed to calculate ozone contactor effluent oocyst concentrations via eq 7. The percent inactivation of *Cryptosporidium* assuming a summer intake temperature of 15°C and CT value of 2.5 is thus predicted to be 60%. Comparable inactivation was assumed following ozonation at the Edgewood treatment. Results will also be presented assuming no inactivation due to ozone.

The low amount of predicted removal due to ozone disinfection was previously identified as a concern (Black and Veatch, 2008). Upgrades to ozone-UV are under design at KGID and are being completed at the Edgewood treatment plant, to achieve 2-3-log inactivation of *Cryptosporidium* with UV disinfection per LT2 requirements (Pearson, 2014; Anderson, 2014). Following any predicted reductions in viable oocyst concentrations due to ozonation, 2- and 3-log reductions for UV disinfection were applied to calculate final treated drinking water concentrations.

3.5 Risk Calculations

Daily exposure to the consumer was then calculated based on the concentration of pathogen in treated water and the volume of water consumed per day, assumed to be 2 L/day (Regli *et al.*, 1991; Haas *et al.,* 1996). The short storage time of treated water is not predicted to result in significant further reductions in oocyst concentrations (<1-2%).

The probability of contracting infection or illness due to *Cryptosporidium* was determined using an exponential dose-response model (Haas et al., 1996), which assumes that the daily probability of infection, P_i, is given by:

$$P_i = 1 - exp(-rN) \tag{3.9}$$

where *r* is a parameter describing the dose-response curve and *N* is the exposure (*e.g.*, number of oocysts). A best fit value of *r* of 0.0042 (Haas et al., 1996) was used in the prior study (Black and Veatch, 2008) and also used here. The annual risk of infection was calculated from the daily probability using the relationship (Yates *et al.*, 1997):

$$P_d = 1 - (1 - P_i)^d \tag{3.10}$$

where *d* is the number of days of exposure (here assumed to be 365). This approach excludes any acquired immunity from a previous exposure, or "herd immunity" (Casman et al., 2000) and is also simpler than the approach used by Eisenberg and others (e.g., Eisenberg et al., 1996), but is consistent with the approach adopted by the USEPA and used in prior studies.

3.6 Results

Model simulations indicated that strong seasonal and diurnal variations in *Cryptosporidium* concentrations can be found near the KGID and Edgewood intakes. The

concentration of *Cryptosporidium* at the intakes due to body-contact recreation in an arbitrary simulation reveals dramatic variations in the levels there (e.g., Fig. 3.6). Oocysts were present only during the summer recreational season, and varied strongly; in this simulation, concentrations ranged from <0.001 to 0.7 oocysts/100 L at the KGID intake, while lower concentrations were predicted at the Edgewood intake (Fig. 3.6). The very sharp increases found on several dates are attributed to AFRs or other large loading events, with the plume rapidly transported past the intake.
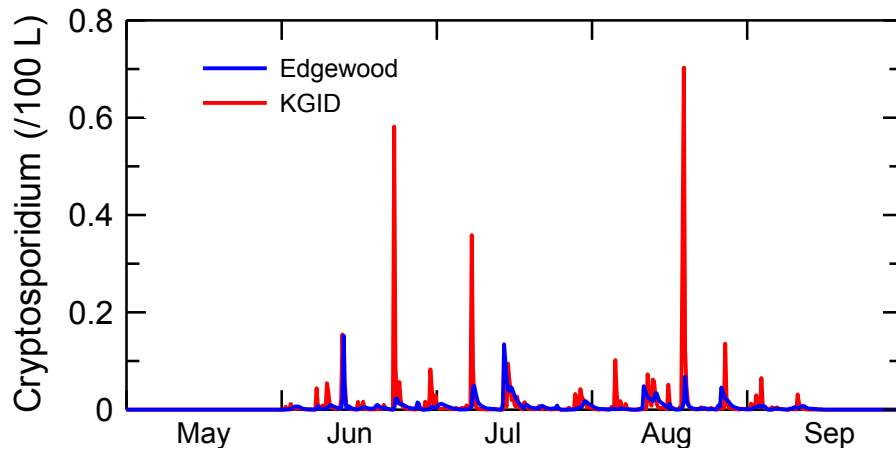

Fig. 3.6. Predicted Cryptosporidium concentrations at KGID and Edgewood intakes (arbitrary simulation).

Concentrations were often, but not exclusively, lower at the Edgewood intake when compared with KGID. The greater distance from shore and from beach areas generally allowed for more loss and dilution, although source areas and transport processes influenced predicted concentrations in complex ways. For example, in the simulation depicted in Fig. 3.6, two events were identified when Edgewood intake concentrations exceeded 0.1 oocysts/100 L and also exceeded those at KGID, while 3 separate events yielded high concentrations at KGID but had negligible effect on concentrations at Edgewood intake (Fig. 3.6). Advective currents to the NNW (Fig. 3.2) and dispersion often rapidly transported oocysts away from this region of the lake.

Detailed information about hydrodynamics and transport are provided in chapter 2; Fig. 3.7 provides a few snapshots from an arbitrary simulation showing oocyst loading, dispersion and transport over time. Beach areas are shown here as light sand-colored squares, while intakes are represented by deep rust red circles. One notices a plume of low concentration (<0.003 oocysts/100 L) at the southern end of the computational domain adjacent to the Lakeside beaches at noon (Fig. 3.7); this is due to a release of pathogens on a previous day. A pulse of oocysts at Nevada Beach yielded a local concentration of almost 1 oocyst/100L that is advected to the north and dispersed laterally.
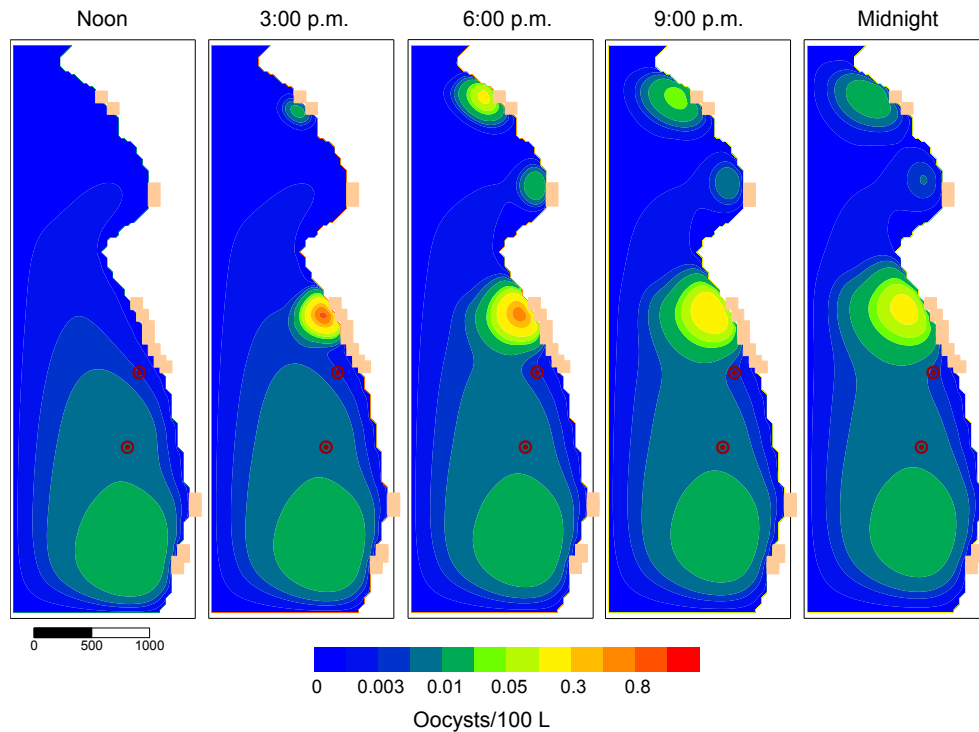
Fig. 3.7. Predicted Cryptosporidium concentrations near KGID and Edgewood intakes over time (arbitrary simulation).

Simulations with recreation at Beach Club and Edgewood Lodge/Resort were compared with earlier risk assessment results. Simulations yielded a >4x increase in the median annual and median summer-average concentrations at the KGID intake compared with findings reported in Black and Veatch (2008) (Table 3.2). The predicted increase at the intake is due to both increased recreational use and the finer-scale grid and improved understanding of the hydrodynamics. To assess the impact of the new model grid and improved hydrodynamics, a separate set of 500 simulations were run using the number and distribution of body-contact recreators as in the original risk assessment. Much of the predicted increase could be attributed to model improvements, with an increase of 0.0016 oocysts/100 L attributable to recreational use at Beach Club and Edgewood Lodge/Resort (Table 3.2). While such increases would be very significant for the original KGID ozone-plant, the upgraded LT2-plant with UV disinfection has ample disinfection capabilities (Fig. 3.8).

Table 3.2. Median predicted annual and summer-average *Cryptosporidium* concentrations at KGID intake.			
Concentration	Black & Veatch (2008)	Original beach use + updated model	Increased beach use+updated model
Annual Average Conc (#/100 L)	0.0018	0.0066	0.0082
Summer-Average Conc (#/100 L)	0.0058	0.0236	0.0293

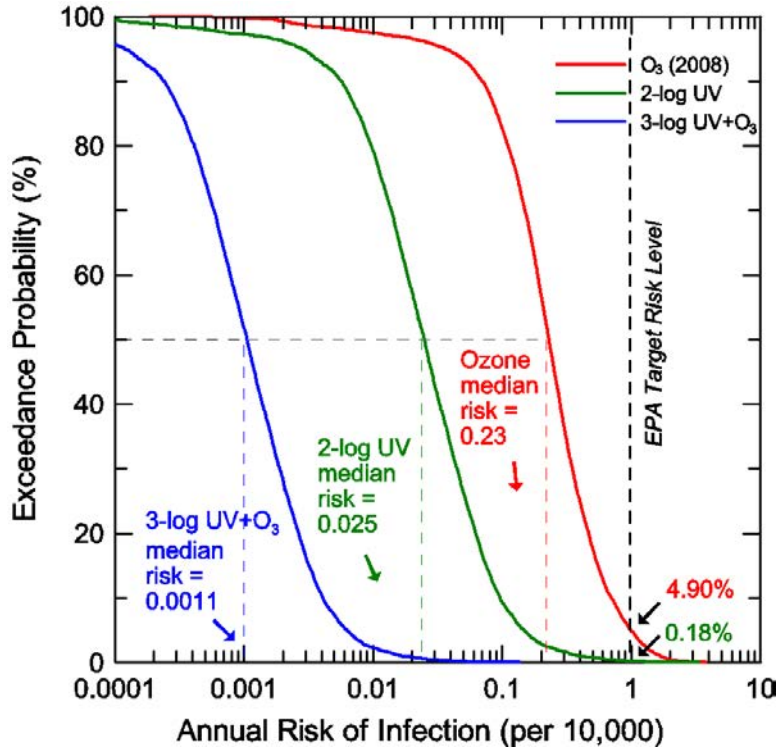Flow Modeling and Pathogens
PO # S004422

Fig. 3.8. Exceedance probability describing annual average risk of infection due to cryptosporidiosis for KGID. Results for O_3 alone (Black & Veatch, 2008) (red line), 2-log treatment with UV (green line), and 3-log treatment with O_3 (blue line).

Three-log UV with limited ozone disinfection substantially lowered the finished drinking water concentration and, with application of the dose-response model, yielded a median annual risk of infection of 0.0011 infections/10,000/yr, a value that was <0.5% of that for ozone alone (0.23 infections/10,000/yr) (Black and Veatch, 2008) (Fig. 3.8). Moreover, the probability of exceeding the USEPA target of 1 infection/10,000/yr was reduced from 4.9% to <0.02% (the lowest possible probability based upon the number of simulations) (Fig. 3.8, blue line). That is, under no simulation out of >5000 did the risk of infection exceed 1/10,000/yr. The highest value reached was only 0.13 infections/10,000/yr. Reduction in treatment to 2-log UV disinfection with no credit for ozone shifted the exceedance probabilities to higher annual risk levels, with the median annual risk of infection rising from 0.0011 to 0.025 infections/10,000/yr. While a finite but very low probability of exceeding the USEPA target was predicted with 2-log UV treatment (0.18%), one notes this value is >27-fold lower than predicted for the original ozone plant (Black & Veatch, 2008).

Simulation results for the Edgewood ozone+UV plant with 3-log UV credit yielded an even lower median annual risk of infection (0.0007 infections/10,000/yr) (Fig. 3.9, blue line). As with KGID, no simulation exceeded the USEPA target annual risk level (highest value of 0.08 infections/10,000/yr), so the probability of exceeding the target as a result of body-contact recreation with ozone+3-log UV treatment is considered to be negligibly small. Reduction in treatment to 2-log UV inactivation and assuming no ozone credit shifted the median risk from

Flow Modeling and Pathogens
PO # S004422

0.0007 to 0.0155 infections/10,000/yr, and yielded a very small (0.04%) probability of exceeding the USEPA target of <1 infection/10,000/yr (Fig. 3.9, green line).
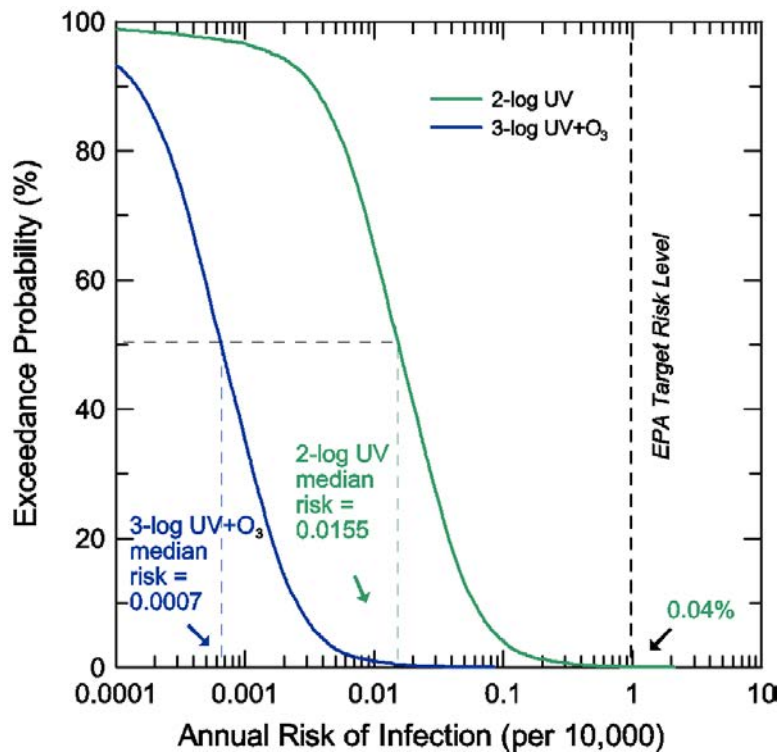

Fig. 3.9. Exceedance probability describing annual average risk of infection due to cryptosporidiosis for Edgewood Water Company. Results for 2-log UV disinfection (green line), and 3-log UV disinfection with O₃ (blue line).

3.7 Assumptions and Model Limitations

Although the models incorporated known input, transport and loss processes to describe *Cryptosporidium* near the intakes, as well as removal at the treatment plants, some assumptions and simplifications were necessarily in place. For example, following previous modeling efforts, natural UV-inactivation within the water column was not included. If the extent of natural UV-inactivation is confirmed to be significant in Lake Tahoe, this would increase net removal within the water and would thus lower predicted *Cryptosporidium* concentrations and associated risk levels.

At the same time, other inputs of oocysts to the lake were not accounted for. For example, dogs and other warm-blooded mammals such as deer can also be a significant source of oocysts to natural waters. Beach surveys documented the presence of a large number of dogs at many of the beaches, and deer and other wildlife could serve as a substantial source of pathogens within the watershed. Inputs from sewerage failures and other less common events could also greatly increase short term loading of pathogens near drinking water intakes. These additional inputs would potentially increase concentrations and corresponding public health risks. Thus, two

Flow Modeling and Pathogens
PO # S004422

potentially important processes were not incorporated into this analysis. There exists some reasonable prospect for these additional inputs of pathogens to be at least partially offset by potential additional loss via natural UV-inactivation, so inclusion of these processes, while theoretically possible, may not substantively alter study conclusions.

Projections were necessarily also made as to the intensity of use at the Beach Club and Edgewood Lodge/Resort beaches, with an estimated 30,000 visitors annually to these new beaches, and one-half of these individuals participating in body-contact recreation. The model is sensitive to projected recreational use (Anderson et al., 1998). Since there is some uncertainty about actual beach attendance, recreational use for any given simulation was drawn from a Gaussian distribution about the mean projected value with a standard deviation estimated at 0.2x the mean. Additional simulations were conducted in which regional annual body-contact recreation was increased up to almost 4x the projected regional use of 74,688/yr (Fig. 3.10). For these higher levels of use, a reduced number of simulations (500) were conducted for each scenario. While the median and general distribution of risk is properly represented, the "tails" of the distribution representing rare combinations of conditions are not necessarily adequately captured. Predicted concentrations at the intake and annual risk of infection were found to scale approximately linearly with intensity of body-contact recreational use across the region (*e.g.*, Fig. 3.10). With 3-log UV inactivation and some limited disinfection with ozone, regional body-contact recreation could be increased to nearly 300,000/yr and the median risk of infection would only increase to 0.0046 infections/10,000/yr for KGID and 0.0028 infections/10,000/yr for Edgewood Water Company. Even with only 2-log UV inactivation and 4x greater use than projected, the probability of KGID exceeding the USEPA target of 1 infection/10,000/yr is estimated to be <0.8%, Given the high degree of treatment achieved at the upgraded drinking water treatment plants, greater levels of recreational use beyond those assumed in these simulations would thus not substantively increase consumer public health risks or the probability of exceeding the USEPA target of 1 infection/10,000/yr.
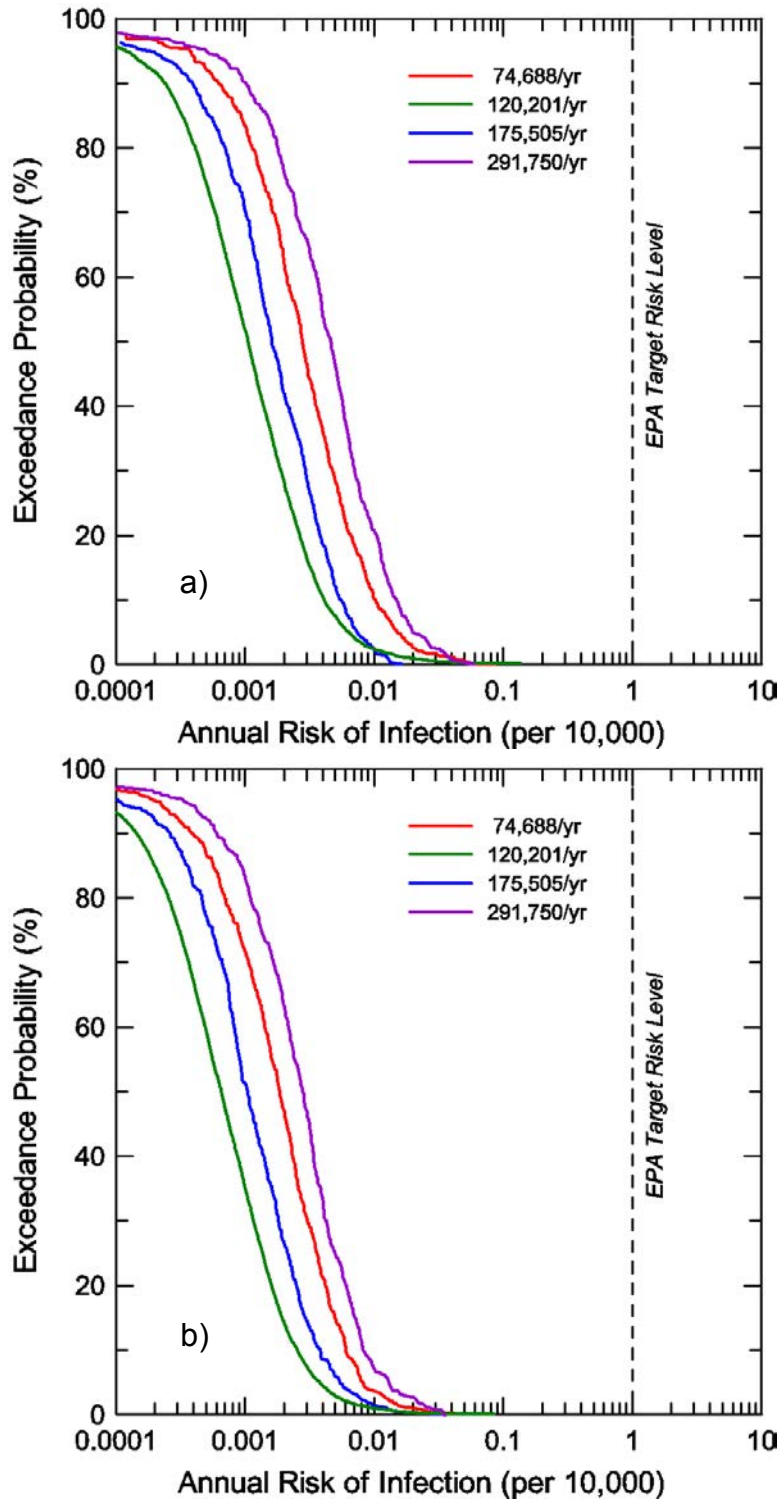
Fig. 3.10. Exceedance probability describing annual average risk of infection due to cryptosporidiosis, with higher levels of body-contact recreational use, for a) KGID and b) Edgewood Water Company assuming 3-log UV disinfection with O₃. Curves would be shifted to the right by about 1.3 logs for 2-log UV inactivation and no O₃ credit.

Flow Modeling and Pathogens

PO # S004422

3.8 Conclusions

Recreational use at Beach Club and Edgewood Lodge/Resort in conjunction with improved hydrodynamics and model segmentation yielded increased predicted *Cryptosporidium* concentrations at the KGID intake compared with earlier calculations (Black and Veatch, 2008), although the treatment plant upgrade with addition of UV disinfection easily handled higher concentrations, and was predicted to reliably deliver finished water with negligible levels of *Cryptosporidium* and by extension other microbial contaminants. The Edgewood intake was further from source areas and predicted to have about 40% lower concentrations and risk levels. Overall risk of infection was very low, with body-contact recreation not representing a significant threat to consumer public health due to the enhanced capabilities of the LT2-compliant drinking water treatment plants.

3.9 References

Amin, O.M. 2002. Seasonal prevalence of intestinal parasites in the United States during 2000. *Am. J. Trop. Med. Hyg.* 66:799-803.

Anderson, M.A., M.H. Stewart, M.V. Yates and C.P. Gerba. 1998. Modeling the impact of body-contact recreation on pathogen concentrations in a source drinking water reservoir. *Water Res.* 32:3293-3306.

Anderson, M.A. 2004. *Predicted Consumer Risk Levels Resulting from Body-Contact Recreation in Agate Bay, Lake Tahoe.* Final Report to the North Tahoe Public Utilities District. 31 pp.

Anderson, R.O. 2014. Edgewood water treatment plant information. Pers. Comm. (email dated January 30, 2014).

Bennett, J.V. S.D. Homberg, M.F. Rogers, and S.L. Solomon. 1987. Infectious and parasitic diseases. *Am. J. Prev. Med.* 55:104-114.

Black and Veatch. 2008. *Lake Tahoe Source Water Protection Risk Assessment.* Final Report. B&V Project No. 41717. 108 pp + Appendices.

Calderon, R.L., E.W. Mood and A.P. Dufour. 1991. Health effects of swimmers and nonpoint sources of contaminated water. *Intern. J. Environ. Health Res.* 1:21-31.

Casman, E.A., B. Fischhoff, C. Palmgren, M.J. Small and F. Wu. 2000. An integrated risk model of a drinking water-borne cryptosporidiosis outbreak. *Risk Anal.* 20:495-511.

Chapra, S.C. 1997. *Surface Water-Quality Modeling.* McGraw-Hill, New York, NY. 844 pp.

Craik, S.A., D. Weldon, G.R. Finch, J.R. Bolton and M. Belosevic. 2001. Inactivation of *Cryptosporidium parvum* oocysts using medium- and low-pressure ultraviolet radiation. *Water Res.* 35:1387-1398.

Eisenberg, J.N., E.Y.W. Seto, A.W. Olivieri and R.C. Spear. 1996. Quantifying water pathogen risk in an epidemiological framework. *Risk Anal.* 16:549-563.

Frost, F.J., T. Muller, R.L. Calderon and G.F. Craun. 2000. A serological survey of college students for antibody to *Cryptosporidium* before and after introduction of a new water filtration plant. *Epidemiol. Infect.* 125:87-92.

Frost, F.J., T. Muller, G.F. Craun, R.L. Calderon and P.A. Roefer. 2001. Paired city *Cryptosporidium* serosurvey in the southwest USA. *Epidemiol. Infect.* 126:301-307.

Haas, C.N., C.S. Crockett, J.B. Rose, C.P. Gerba and A.M. Fazil. 1996. Assessing the risk posed by oocysts in drinking water. *J. Am. Water Works Assoc.* 88:131-136.

Hoyer, A.B., S.G. Schladow and F. Rueda-Valdivia. 2014. Local dispersion of invasive bivalve species by wind-driven lake currents. *Limnol. Oceanogr.: Fluids Environ.* (in review).

Kramer, M.H. B.L. Herwaldt, G.F. Craun, R.L. Calderon and D.D. Juranek. 1996. Waterborne disease: 1993 and 1994. *J. Am. Water Works Assoc.* 80:66-80.

Martin, J.L and S.C. McCutcheon. 1999. Hydrodynamics and Transport for Water Quality Modeling. Lewis Publ., Boca Raton, FL. 794 pp.

Medema, G.J., F.M. Schets, P.F.M. Teunis and A.H. Havelaar. 1998. Sedimentation of free and attached *Cryptosporidium* oocysts and *Giardia* cysts in water. *Appl. Environ. Microbiol.* 64:4460-4466.

Ong, C., W. Moorehead, A. Ross, and J. Isaac-Renton. 1996. Studies of *Giardia* spp. and *Cryptosporidium* spp. in two adjacent watersheds. *Appl. Environ. Microbiol.* 62:2798-2805.

Pearson, W. 2014. KGID water treatment plant information. Pers. Comm. (email dated Dec. 30, 2013).

Regli, S., J.B. Rose, C.N. Haas and C.P. Gerba. 1991. Modeling the risk of *Giardia* and viruses in water. *J. Am. Water Works Assoc.* 83:76-84.

Rose, J.B., R.L. Mullinax, A.N. Singh, M.V. Yates and C.P. Gerba. 1987. Occurrence of rotaviruses and enteroviruses in recreational waters at Oak Creek, Arizona. *Water Res.* 21:1375-1381.

Rueda, F.J., S.G. Schladow and S.O. Palmarsson. 2003. Basin-scale internal wave dynamics during a winter cooling period of a large lake. *J. Geophys. Res.* 108:42-1 - 42-16.

Soave, R. and C.S. Weikel. 1990. *Cryptosporidium* and other protozoa including *Isopora, Sarocysts, Balantidium coli* and *Blastocysts*. In *Principles and Practice of Infectious Diseases*, eds. G.L. Mandell, R.G. Douglas and J.E. Bennett, pp.2122-2130. Churchill Livingstone, Inc., New York.

Steissberg, T.E., S.J. Hook and S.G. Schladow. 2005. Measuring surface currents in lakes with high spatial resolution thermal infrared imagery. Geophys. Res. Lett. 32:L11402.

Stewart, M.H, M.V. Yates, M.A. Anderson, C.P. Gerba, J.B. Rose, R.DeLeon and R.L. Wolfe. 2002. Predicted public health consequences of body-contact recreation on a potable water reservoir. *J. Am. Water Works Assoc.* 94:84-97.

Sunderland, D., T.K. Graczyk, L. Tamang and P.N. Breysse. 2007. Impact of bathers on levels of *Cryptosporidium parvum* oocysts and *Giardia lambia* cysts in recreational beach waters. *Water Res.* 41:3483-3489.

Tahoe Environmental Research Center (TERC). 2013. *Tahoe: State of the Lake Report.* UC Davis. 82 pp.

Thomann, R.V. and J.A. Mueller. 1987. Principles of Surface Water Quality Modeling and Control. Harper and Row Publishers, New York.

Ungar, B.L. 1990. Cryptosporidiosis in humans (Homo sapiens). In *Cryptosporidiosis in Man and Animals*, eds. J.P. Dubey, C.A. Speer and R. Fayer. pp. 59-82. CRC Press, Boca Raton, FL.

USEPA. 1997. Removal of Cryptosporidium and Giardia through Conventional Water Treatment and Direct Filtration. EPA/600/SR-97-026. 9 pp.

Walker, F.R. and J.R. Stedinger. 1999. Fate and transport model of *Cryptosporidium*. *J. Environ. Eng.* 125:325-333.

Yates, M.V., M.A. Anderson, C.P. Gerba and J.B. Rose. 1997. *The Impact of Body-Contact Recreation in the Eastside Reservoir Project on 1) Pathogen Risk to Consumers and Recreators and 2) MTBE Contamination.* Final Report to the Metropolitan Water District of Southern California. 93 pp. + Appendices.

4. Potential Transport of Herbicides and Pesticides

4.1 Introduction

Environmental regulations in Lake Tahoe are extremely stringent, and currently there is a prohibition on the use of herbicides, pesticides and similar chemicals in the lake. Recently, permitting the use of herbicides for the treatment of Eurasian watermilfoil in Tahoe Keys has been under consideration by the Lahontan Regional Water Quality Control Board. Although no decision has been made to date, there is interest on the possible fate of herbicides or their breakdown products should their use be permitted and in the event that they escape from the Tahoe Keys.

Utilizing the particle tracking model described in Chapter 2, a limited number of simulations were conducted to look at where in the lake herbicides would travel to, and to assess whether they posed a risk for water purveyors.

4.2 Methods

The distribution of herbicides released at Tahoe Keys was studied using the hydrodynamic model and 3D particle tracking model described in Chapter 2. One hundred neutrally-buoyant particles were released at a point just outside the Tahoe Keys every hour during a ten day period, July 26 until August 3 (day 206–216) of 2008. That represented a total of 24,000 particles, and was meant to simulate a small, continuous release of herbicide from the Tahoe Keys. The initial particle cloud was normally-distributed, centered at P1 (Fig.1) with a standard deviation of 10m and 0.5m in the horizontal and vertical, respectively. These particles were free to move with the water current induced by winds and convection. The input prediction for current speed, current direction and vertical turbulence in the 3D domain had previously been output by the hydrodynamic code at a time step of 1 hour and was then interpolated to the particle code time step. The particle time step was set to 10s, to satisfy the convergence criterion for particle tracking simulations proposed by Ross and Sharples (2004). The particles' position was tracked for a time period of 1 day.

4.3 Results

The simulated herbicide released at Tahoe Keys (P1, Fig.1) were dispersed by the wind-induced near-shore currents. The dispersion occurred along three discrete preferential pathways: (1) toward the east contained by the 2m depth contour, (2) toward the northeast over open water, and (3) toward the west along the shoreline. Dispersion along pathway 1 was driven by the predominant coast jet induced by episodically strong wind forcing from the southwest. Pathway 2 is most likely the result of the interplay between the local near-shore circulation and the basin-scale circulation. The southern basin-scale gyre is anticyclonic (counter-clockwise) with northeast flow at the longitude of P1. Local current, in turn, may be deviated toward the north by the complex near-shore bathymetry as well as weak to intermediate SE wind during the night. To a lesser extent, herbicide may be dispersed toward the west driven by westward alongshore currents. These currents are induced by intermediate NW winds. The depth distribution of vertical herbicide position after 1 day of simulation (Fig.2) reveals that >79% of the simulated herbicides remains within the upper 2m of the water column. This is significant as it means that the beaches along the south shore of Lake Tahoe would be the areas most directly affected.
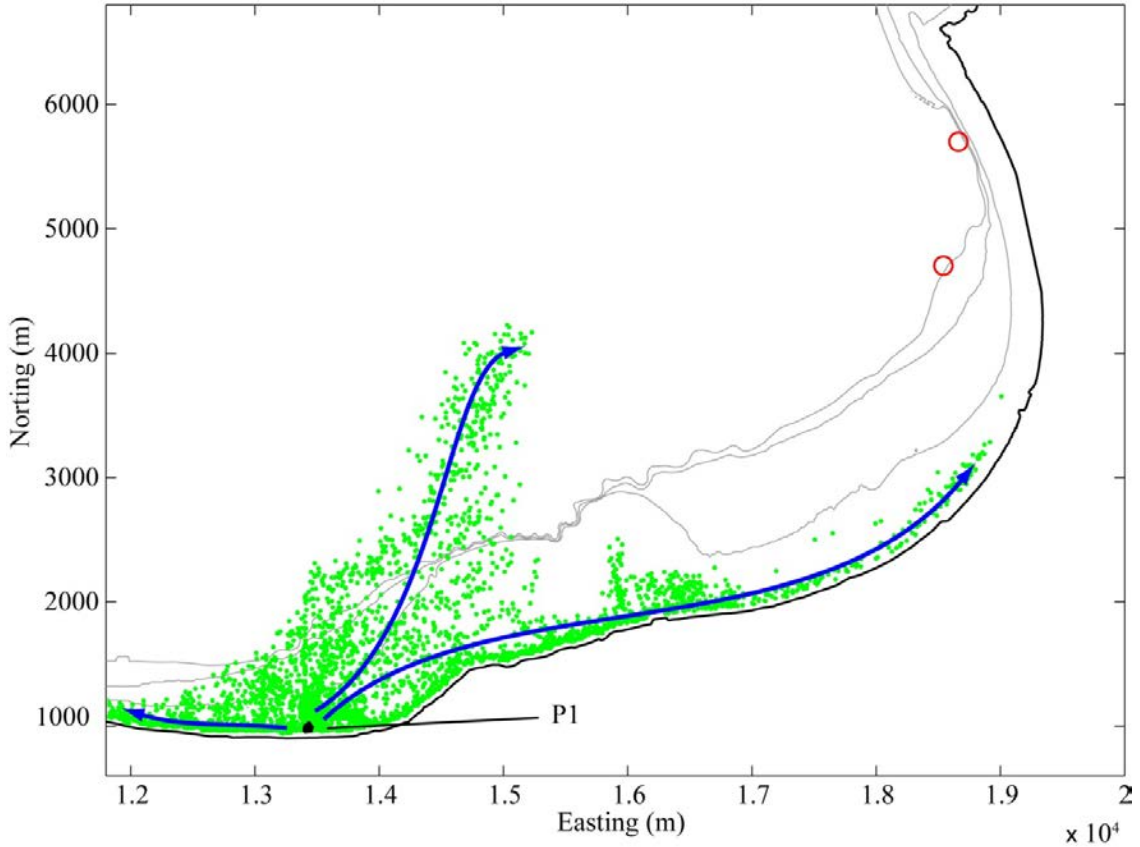
Figure 1. Dispersion pathways of simulated herbicide released at Tahoe Keys (P1). Green dots mark final herbicide distribution for all of the 24 hour simulations during the ten day study period. Red circles mark location of Edgewood and Kingsbury Gate intake. Blue arrows mark dispersion pathways. Gray lines denote the depth contours (2, 5 and 10m) for reference.
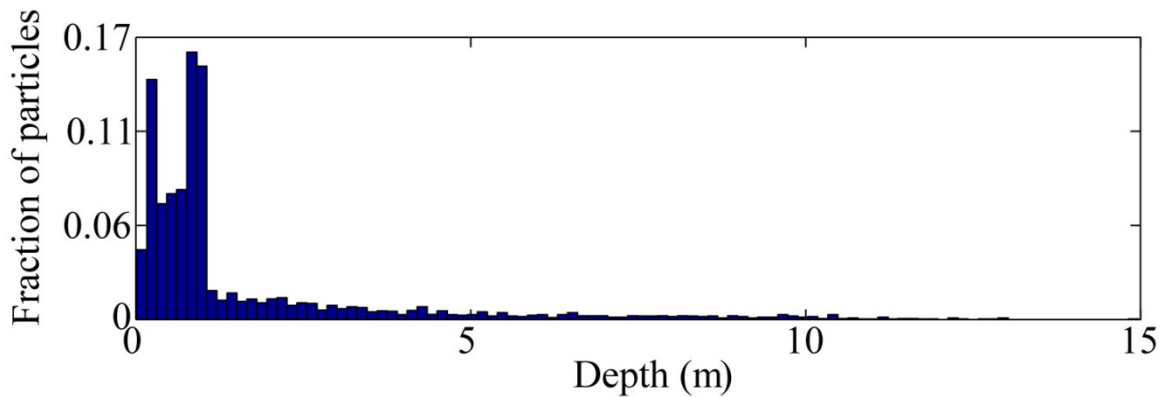

Figure 2. Depth distribution of simulated herbicide expressed as fraction of total particle released.

4.4 Conclusions

The results indicate that a release of a surrogate for herbicide (neutrally buoyant particles) or any other constituent from the vicinity of Tahoe Keys has the potential to reach the shoreline areas in the south-east and the south west of the lake within a 24 hour period. Most of the material would be confined to a depth of less than 2 m during the first 24 hours. For the case of the south-east portion, the particles then would be subject to the transport processes described in Chapter 2, and have a significant probability of reaching drinking water intakes within 48 hours of release.

It must be borne in mind that these results are a first estimate of the fate of herbicides. No account has been taken of the dilution that a real plume of herbicide would be subject to, and the possible breakdown into other chemicals. Likewise the toxicity (if any) of the herbicide for the case of consumption or body contact recreation has not been considered as it was beyond the scope of the study. However, should the use of herbicides be permitted at Lake Tahoe, there is a strong case that a more complete study of the fate of these products on public health should be undertaken.

4.5 References

Ross, O.N. and J. Sharples (2004) Recipe for 1-D Lagrangian particle tracking models in space-varying diffusivity. Limnol. Oceanogr.: Methods, 2: 289-302.